

**Boundary layer flow over a vertical plate with
new Rosseland thermal radiation**



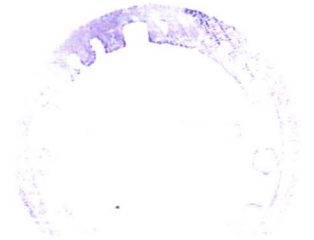
By

Noor Muhammad

Supervised By

Dr. Sohail Nadeem

**Department of Mathematics
Quaid-i-Azam University
Islamabad, Pakistan**



Boundary layer flow over a vertical plate with new Rosseland thermal radiation



By
Noor Muhammad

A THESIS SUBMITTED IN THE PARTIAL FULFILLMENT OF THE REQUIREMENTS FOR THE
DEGREE OF

MASTER OF PHILOSOPHY

IN

MATHEMATICS

Supervised By

Dr. Sohail Nadeem

Department of Mathematics

Quaid-i-Azam University

Islamabad, Pakistan

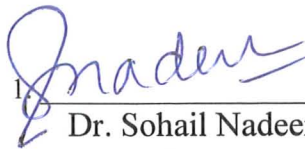
2015


Boundary layer flow over a vertical plate with new
Rosseland thermal radiation
By


Noor Muhammad
CERTIFICATE

A THESIS SUBMITTED IN THE PARTIAL FULFILLMENT OF THE
REQUIREMENTS FOR THE DEGREE OF THE MASTER OF PHILOSOPHY

We accept this dissertation as conforming to the required standard


1. _____
Dr. Sohail Nadeem
(Supervisor)


2. _____
Prof. Dr. Tasawar Hayat
(Chairman)


3. _____
Dr. Muhammad Salahuddin
(External Examiner)

Department of Mathematics
Quaid-I-Azam University
Islamabad, Pakistan
2015

Acknowledgments

In the name of ALLAh, the most Beneficent, Who enabled me to complete my dissertation. I offer my humble gratitude to Holy Prophet MUHAMMAD (peace Be Upon Him), who is forever a touch of guidance and knowledge for humanity as a whole.

I feel highly privileged to express my heartfelt gratitude to my supervisor, Dr. Sohail Nadeem for his skilful guidance, helpful suggestions and inspiring attitude during the research. His kindness and generous response to my difficulties during the research work to complete the dissertation in time will never forgotten.

I am also thankful to all the teaching staff of our department. Their inspiration and suggestions helped me to complete my research work.

I would like to extend my sincere gratitude to my friends, Muhammad Farooq, Arif Ullah khan, Massod Shah, Ikram Ullah and Waheed Ahmad Khan who have supported me and given me confidence to complete this task.

At the end, my appreciation is also expressed to my parents, brothers and other family members for their constant support, love, guidance and encouragement throughout my career.

Noor Muhammad

July 2015.

Preface

Thermal radiation is the transfer of energy by means of photons in electromagnetic waves. Radiation heat transfer can occur in any transparent medium (solid or fluid) or through a vacuum. Heat transfer by simultaneous radiation and convection has applications in numerous technological problems, including combustion, furnace design, nuclear reactor safety, fluidized bed heat exchangers, solar ponds, solar collectors, turbid water bodies, photochemical reactors and many others [1]. Solar energy is probably the most suitable source of renewable energy that can meet the current energy requirements. The energy obtained from nature in the form of solar radiations can be directly transformed into heat and electricity. Researchers concluded that with the addition of nanoparticles in the base fluids, heat transfer and the solar collection processes can be improved. Buongiorno [2] developed the nonhomogeneous equilibrium mathematical model for convective transport of nanofluids. He concluded that Brownian motion and thermophoretic diffusion of nanoparticles are the most important mechanisms for the abnormal convective heat transfer enhancement.

Smith was the first who proposed the effect of radiation in a boundary layer flow [3]. Viskanta and Grosh [4] considered the effects of thermal radiation on the temperature distribution and the heat transfer in an absorbing and emitting medium, flowing over a wedge (Falkner-Skan flow), using the Rosseland approximation. As Viskanta and Grosh [3] noted that the thermal radiation becomes an additional factor in hypersonic flight, missile reentry, rocket combustion chambers, power plants for interplanetary flight and gas cooled nuclear reactors.

Subsequently, a huge amount of papers have been published in the literature on the stimulus of radiation in boundary layer flows including the work of some researchers mentioned in [5-9]. The exposed literature is now very gorgeous including cases with moving plates, suction or injection [10, 11], magnetohydrodynamics, porous media, viscous dissipation, thermophoresis, variable fluid properties, chemical reaction, non-Newtonian fluids, micropolar fluids and so many more works were done.

Pantokratoras studied the natural convection along a vertical isothermal plate with linear and nonlinear Rosseland thermal radiation [12]. Hossain et al. [13], reported the effects of radiation on free convection from a porous vertical plate. Nonlinear radiation heat transfer effects in the natural convective boundary layer flow of nanofluid past a vertical plate were investigated by Hayat et al. [14]. Investigations in the thermal radiations and nanofluid flows have received remarkable popularity in research community in last couple of decades primarily due to their variety of applications in power generation, in transportation where nanofluid may be utilized in vehicles as coolant, shock absorber, fuel additives etc., in cooling and heating problems which may involve the use of nanofluids for cooling of microchips in computer processors, in improving performance efficiency of refrigerant/air-conditioners etc. and in biomedical applications in which magnetic nanoparticles may be used in medicine, cancer therapy and tumor analysis. The above mentioned studies were confined to the linear radiative heat transfer effects which are only valid for small temperature differences. The present work deals with the natural convection flow of an electrically conducting nanofluid past a vertical plate in the presence of nonlinear thermal radiation.

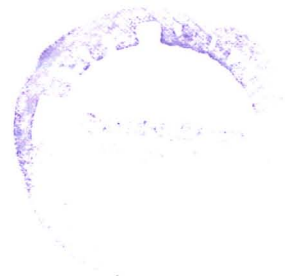
Commonly the governing equations describing thermal radiations flows are nonlinear. For a highly nonlinear equation it is not easily possible to obtain an exact solution. So, analytic methods are used to obtain the results of physical interest. Optimal Homotopy Analysis Method (OHAM) [15-18] has been widely used to solve nonlinear differential equations. This method provides us freedom for the choice of linear operator and with the help of auxiliary parameter we can control the convergence of the obtained solution.

In present dissertation, we have considered the natural convection flow of an electrically conducting second grade [19-23] nanofluid past a vertical plate in the presence of nonlinear thermal radiation. Mathematical model proposed by Buongiorno [2] is adopted. The governing equations are first simplified by using similarity transformations and then OHAM is used to obtain the solution. Tables and graphs are drawn to explain the behaviour of flow field.

This dissertation consists of three chapters, in chapter one, we have discussed some basics of fluid mechanics and the basic equations need for the study of fluid.

In chapter two we have review the work of A. Pantokratoras [12].

In chapter three we have extended the work of Ref [12] for mixed convection second grade nanofluid flow in presence of thermal radiation. The solutions of the equations is computed by optimal homotopy analysis method (OHAM). The results, graphs and discussion of various parameters appeared in the model are also listed in chapter three. The concluding remarks are presented at the end of the chapter.



Contents

1	Basic definitions	4
1.1	Fluid	4
1.2	Fluid mechanics	4
1.2.1	Fluid statics	4
1.2.2	Fluid dynamic	5
1.3	Stress	5
1.3.1	Shear stress	5
1.3.2	Normal stress	5
1.4	Strain	5
1.5	Viscosity	5
1.5.1	Kinematic viscosity (ν)	6
1.6	Flow	6
1.6.1	Laminar flow	6
1.6.2	Turbulent flow	6
1.7	Newtonian's law of viscosity	7
1.8	Newtonian fluids	7
1.9	Non-Newtonian fluids	7
1.9.1	Differential type	8
1.9.2	Second grade fluid	8
1.9.3	Third grade fluid	8
1.10	Mechanism of heat flow	9
1.10.1	Conduction	9

1.10.2	Convection	9
1.10.3	Forced convection	10
1.10.4	Natural convection	10
1.10.5	Mixed convection	10
1.10.6	Radiation	10
1.11	Thermal conductivity	11
1.12	Thermal diffusivity	11
1.13	Newtonian heating	11
1.14	Dimensionless numbers	12
1.14.1	Reynolds number	12
1.14.2	Prandtl number	12
1.14.3	Grashof number	13
1.14.4	Deborah number	13
1.14.5	Nusselt number	13
1.14.6	Skin friction	14
1.14.7	Sherwood number	14
1.15	Some basic equations	15
1.15.1	Continuity equation	15
1.15.2	Equation of motion	15
1.15.3	Energy equation	15
1.15.4	Concentration equation	17
1.16	Homotopy analysis method	17
2	Natural convection along a vertical isothermal plate with linear and non-linear Rosseland thermal radiation	19
2.1	Introduction	19
2.2	Mathematical formulation	20
2.3	Solutions by the homotopy analysis method	23
2.3.1	Zeroth order problem	23
2.3.2	k th-order deformation problems	24
2.4	Analysis of the solutions	25

2.4.1	Convergence of the series solution	25
2.4.2	Discussion	26
2.5	Concluding Remarks	29
3	MHD Flow of a Second Grade Nanofluid with Thermal radiation	30
3.1	Introduction	30
3.2	Mathematical model	30
3.3	Homotopy analysis solutions	36
3.4	Convergence of the homotopy solutions	39
3.5	Results and discussions	40
3.6	Concluding Remarks	48

Chapter 1

Basic definitions

This chapter contains some essential definitions, concepts and laws, which are beneficial for the thoughtful of analysis accessible in the consequent chapters.

1.1 Fluid

Fluid is a material that deforms constantly under the influence of shear stress, no matter how slight the shear stress may be or fluid is a material which cannot tolerate a shear force under the static condition.

1.2 Fluid mechanics

The branch of mechanics which deals with the performance of all kind of fluids moreover at rest or in motion and also the effects of fluid properties on boundaries. In other words, fluid mechanics is a branch of continuous mechanics which describes the effects of forces on fluid particles in motion and under the static condition in a continuous material. It is divided into two main branches.

1.2.1 Fluid statics

It is the branch of fluid mechanics which describes the behavior of fluids under static (at rest) condition.

1.2.2 Fluid dynamic

It is the branch of fluid mechanics which exhibits the behavior of fluids in motion.

1.3 Stress

The force acting on the surface of unit area within a deformable body is known as stress. In SI system the unit of stress is $kg/m.s^2$ and dimension $[\frac{M}{LT^2}]$. Further stress is divided into the shear stress and normal stress components.

1.3.1 Shear stress

In shear stress the force acting parallel to the unit surface area.

1.3.2 Normal stress

In normal stress the force acting perpendicular to the unit surface area.

1.4 Strain

Strain is a dimensionless quantity used to measure the deformation of an object caused by the applied forces.

1.5 Viscosity

It is the internal property of fluid that describes the resistance of a fluid against any gradual deformation when distinct forces are acting upon it. Mathematically, it can be written as the ratio of shear stress to the rate of shear strain, i.e.

$$\text{viscosity } (\mu) = \frac{\text{shear stress}}{\text{rate of shear strain}}. \quad (1.1)$$

It is also known as absolute viscosity. In SI system the unit of viscosity is $kg/m.s$ and its dimension $[\frac{M}{LT}]$.

1.5.1 Kinematic viscosity (ν)

The kinematic viscosity (momentum diffusivity) is the ratio of dynamic viscosity μ to the density of the fluid ρ . It is commonly denoted by the Greek letter nu (ν). Mathematically we write in the following form, i.e.

$$\nu = \frac{\mu}{\rho}. \quad (1.2)$$

The unit of kinematic viscosity in SI system is m^2/s and its dimension is $\left[\frac{L^2}{T}\right]$.

1.6 Flow

An object or material tends to deform under the influence of certain forces. If the deformation increases continuously without any limit, then such phenomenon is known as flow.

1.6.1 Laminar flow

The flow in which fluid particles have specific paths and paths of individual particles do not interact or cross each other. If we observe the smoke rising from a cigarette. For the first few centimeters the flow is certainly laminar and after a short interval of time the smoke becomes turbulent.

1.6.2 Turbulent flow

Turbulent flow is the contrast to that of laminar flow and defined as, that type of flow in which fluid particles have no specific paths and also these paths of individual particles cross each other. Example of turbulent flow can be seen from the following.

The turbulence occurred due to convection can be understood by considering that we heat up water in a pot through an electric cooker. Now let wait for a few moments, we will observe that the water has started to exchange in a laminar way, through a proper way. It will start to move in a laminar manner. Let us wait a little bit more, we will see that from the bottom of water bubbles start to rise to the surface due to which the motion of water molecules becomes very difficult or complicated or in simple words it is turbulent. This is the instance of the turbulence occurred through convection.

1.7 Newtonian's law of viscosity

The Newton's law of viscosity describes that shear stress which deforms the fluid element is directly and linearly proportional to velocity gradient.

Mathematically,

$$\tau_{yx} \propto \frac{du}{dy}, \quad (1.3)$$

or

$$\tau_{yx} = \mu \frac{du}{dy}, \quad (1.4)$$

where τ_{yx} is the shear stress acting on fluid element and μ is the constant of proportionality which is known as dynamic viscosity.

1.8 Newtonian fluids

Fluids obeying the Newton's law of viscosity are known as Newtonian fluids, i.e. shear stress is directly and linearly proportional to the deformation rate. Keep in mind that viscosity is constant for each Newtonian fluid at a given temperature and pressure. Examples of Newtonian fluids are Air, water, sugar solutions, glycerin, light-hydrocarbon oils, Kerosene etc.

1.9 Non-Newtonian fluids

The non-Newtonian fluids are those that do not obey the Newton's law of viscosity. Remember that viscosity for such fluids do not remain constant but it varies with the applied shear stress. For such fluids we can write

$$\tau_{yx} \propto \left(\frac{du}{dy} \right)^n, \quad n \neq 1, \quad (1.5)$$

or

$$\tau_{yx} = \eta \frac{du}{dy}, \quad \eta = k \left(\frac{du}{dy} \right)^{n-1}, \quad (1.6)$$

where η is the apparent viscosity, k is the consistency index and n is the index of flow behavior. Here for $n = 1$ above equation reduces to the Newton's law of viscosity. Examples of such fluids are paints, flour dough, ketchup, polymer solutions, tooth paste and blood etc. Further

non–Newtonian fluids are categorized into the three types (i) Integral type (ii) Differential type (iii) Rate type. In this dissertation we only consider the differential type fluids.

1.9.1 Differential type

Fluids of differential type or in a relaxed way Rivlin-Ericksen fluids. In such materials, a tiny portion of the past time of the deformation gradient has an effect on the stress. The incompressible homogeneous fluid of second grade is one of the special sub class that retained in enormous quantity of attention amongst fluids of differential type, and some misunderstanding surrounding general fluids of differential type get up from and is fixed in the misunderstood values of the thermodynamics and the stability of this model.

1.9.2 Second grade fluid

The Cauchy stress tensor for a second grade fluid is defined as

$$\boldsymbol{\tau} = -p\mathbf{I} + \mu\mathbf{A}_1 + \alpha_1\mathbf{A}_1 + \alpha_1\mathbf{A}_2 + \alpha_2\mathbf{A}_1^2,$$

here

$$\begin{aligned}\mathbf{A}_1 &= (\text{grad } \mathbf{V}) + (\text{grad } \mathbf{V})^T \\ \mathbf{A}_2 &= \frac{d\mathbf{A}_1}{dt} + \mathbf{A}_1 (\text{grad } \mathbf{V}) + (\text{grad } \mathbf{V})^T \mathbf{A}_1,\end{aligned}$$

here the Clausius–Duhem inequality is holed and Helmholtz free energy is minimum in equilibrium for the fluid locally at rest when [43]

$$\mu \geq 0, \quad \alpha_1 \geq 0, \quad \alpha_1 + \alpha_2 = 0.$$

1.9.3 Third grade fluid

The Cauchy stress tensor for a third grade fluid is defined as

$$\begin{aligned}\boldsymbol{\tau} &= -p\mathbf{I} + \mu\mathbf{A}_1 + \alpha_1\mathbf{A}_1 + \alpha_1\mathbf{A}_2 + \alpha_2\mathbf{A}_1^2 + \mathbf{S}, \\ \mathbf{S} &= \beta_1\mathbf{A}_3 + \beta_2(\mathbf{A}_2\mathbf{A}_1 + \mathbf{A}_1\mathbf{A}_2) + \beta_1(\text{tr}\mathbf{A}_1^2)\mathbf{A}_1,\end{aligned}$$

in which p is the pressure, \mathbf{I} is the identity tensor, μ is the coefficient of viscosity and α_j ($j = 1, 2$), β_j ($j = 1, 2$) denotes the material constants, \mathbf{A}_j ($j = 1, 2, 3$) the Rivlin–Ericksen tensors, and by the way we can get the higher order grade fluid.

1.10 Mechanism of heat flow

We know that there is a transfer of energy, as heat, between a system and its environment, or when one considers different bodies with different temperature then the heat flows from the body at high temperature to the body at low temperature. Here we discuss how this transfer takes place. This transfer of heat takes place by three methods.

1.10.1 Conduction

The transfer of heat from one end of the body to another end of the body due to the only collision of molecules which are in contact and not due to the transfer of molecules is called conduction. Mathematically, we write

$$q = -kA \left(\frac{\Delta T}{\Delta \eta} \right),$$

where $\frac{\Delta T}{\Delta \eta}$ denotes the temperature gradient along the direction of area A , and k is the thermal conductivity constant and the unit is $W/m.K$.

1.10.2 Convection

In convection the transfer of heat take place due to the relative motion or transfer of molecules of the object or body. For example, if we heat up water, the volume of water at the end will be heat up by conduction from the metallic end and its density reduces. Since it becomes slightly dense, it goes upwards up to the surface of the volume of water and transfers the upper colder and denser mass of water downwards, to the bottom. The mathematics of convection is of the form,

$$q = \xi A (T_f - T_0).$$

Here ξ is for convective heat transfer coefficient, A is the area implied in the heat transfer process, T_f is for the temperature of the system and T_0 is a reference temperature.

1.10.3 Forced convection

A mechanism of heat transfer in which motion of the particle of fluid is produced by an outer source like a pump and fan etc. Forced convection is usually used to increase the rate of heat exchange.

1.10.4 Natural convection

This type of heat transfer arises due to the temperature differences which disturb the density and thus buoyancy of the fluid. Natural convection can only occur in the presence of gravitational field. It is also known as free convection.

1.10.5 Mixed convection

Mixed (combined) convection flow occurs when natural convection and forced convection mechanisms act together to transfer heat.

1.10.6 Radiation

Radiation is that process in which heat is transferred directly by electromagnetic radiations, that involves of particles and waves, i.e. photons and waves, the similar as visible light. Thus, the radiative heat transfer can proceeds through vacuum. For example, if we place an object under the direct sunbeams, after some time the object will be heated. The exchange of heat between objects occurs due to radiation.

In liquids and gases convection and radiation play very important role in the transfer of heat but in solids convection is totally absent and radiation is usually negligible. Thus for solid materials conduction play major role in the transfer of heat. The mathematically the amount of heat transferred by radiation is

$$q = \epsilon\sigma_{SB}A(\Delta T)^4$$

Here q represents the heat transferred by radiation, ϵ is the emissivity of the system, σ_{SB} is the

Stephan-Boltzmann constant whose value is $5.6697 \times 10^{-8}, W/m^2.K^4$, A is the area involved in the heat transfer by radiation, and $(\Delta T)^4$ is temperature the difference between two systems to the fourth or higher power.

1.11 Thermal conductivity

Thermal conductivity is the property of a material that measures the ability to conduct heat. Fourier's law of conduction relates the rate of heat transfer by conduction to the temperature gradient is

$$\frac{dQ}{dt} = -kA \frac{dT}{dx}, \quad (1.7)$$

where $\frac{dQ}{dt}$ is the rate of heat transfer, k is the thermal conductivity, A is the area.

Now we define the thermal conductivity from the Fourier's law as "the rate of heat transfer through a unit thickness of a material per unit area and per unit temperature difference".

Thermal conductivity of most liquids decrease with increasing temperature except water. The unit of thermal conductivity is $kg.m/s^3.K$ and dimension is $\left[\frac{ML}{T^3\theta}\right]$.

1.12 Thermal diffusivity

We define the thermal diffusivity of a material as, "thermal conductivity of a material divided by the product of density and specific heat at constant pressure".

Mathematically, it can be expressed as

$$\alpha = \frac{k}{\rho c_p}. \quad (1.8)$$

The unit of thermal diffusivity in SI system is m^2/s and dimension is $\left[\frac{L^2}{T}\right]$.

1.13 Newtonian heating

This is the heat transfer in which the internal resistance of a substance to flow heat is ignored. Here the rate of heat transfer is directly proportional to the surface temperature of the

substance. Remember that in Newtonian heating the temperature remains same throughout the substance at a given time. Newtonian heating is also known as the lumped heat capacity analysis.

1.14 Dimensionless numbers

1.14.1 Reynolds number

This number is used to check whether the flow is laminar or turbulent. It is denoted by Re. Reynolds number got by comparing inertial force with viscous force. Inertial forces act upon all masses in a non-inertial frame of reference while viscous force is the internal resistance of a fluid to flow.

Mathematically, we have

$$\text{Re} = \frac{\text{Inertial force}}{\text{Viscous force}} \quad (1.9)$$

$$\text{Re} = \frac{\rho v^2/x}{\mu v/x^2} \quad \text{or} \quad \text{Re} = \frac{\rho v x}{\mu}. \quad (1.10)$$

Here v is the fluid velocity, x is the characteristic length and μ is the kinematic viscosity. When Reynolds number is small the viscous forces are dominant which characterize by the laminar flow while turbulent flow occurs at high Reynolds number due to the dominant inertial forces.

1.14.2 Prandtl number

Prandtl number is used to measure the ratio of momentum diffusivity to thermal diffusivity. It is the dimensionless quantity. Mathematically, it can be written as

$$\text{Pr} = \frac{\text{viscous diffusion rate}}{\text{thermal diffusion rate}} \quad (1.11)$$

$$\text{Pr} = \frac{\nu}{\alpha} = \frac{\mu/\rho}{k/\rho c_p} = \frac{\mu c_p}{k} \quad (1.12)$$

where ν is the kinematic viscosity or momentum diffusivity, α is the thermal diffusivity, c_p is the specific heat capacity with unit in SI system as $J/kg K$, and here k is the thermal conductivity having unit in SI system are W/m . Physical significance of Prandtl number is that, it gives the

relative thickness of velocity boundary layer and thermal boundary layer. For small Pr heat diffuses hurriedly as related to momentum.

1.14.3 Grashof number

This is a dimensionless quantity used to investigate the velocity distribution in free convection systems. It defines the relationship between buoyancy force and viscous force exerting on a fluid. which got named after the German engineer Franz Grashof.

Mathematically it can be denoted by the relation,

$$Gr = \frac{\text{buoyant force}}{\text{viscous force}} = g\beta(T - T_\infty)\frac{x^3}{\nu^2}. \quad (1.13)$$

Here g is the gravitational acceleration, β is the volumetric thermal expansion coefficient, x is the characteristic length, ν is the kinematic viscosity and T, T_∞ are the temperature of the fluid and surrounding respectively.

1.14.4 Deborah number

Deborah number De for a material can be defined as the ratio of time of relaxation t_r to time of observation or characteristic time scale t_f . Mathematically it can be written as

$$De = \frac{t_r}{t_f} \quad (1.14)$$

where t_r is the relaxation time and t_f is the characteristic time or time of observation. If the time of relaxation is very small than the time of observation of a material i.e. small Deborah number, material behaves like fluid with an associated Newtonian viscous flow. But on the other hand, if the time of relaxation of a material is large than the time of observation i.e. large Deborah number, then material behaves like solid.

1.14.5 Nusselt number

Nusselt number is basically the dimensionless heat transfer coefficient that defines measure of the ratio of convective to conductive heat transfer through the boundary and can be commu-

icated as

$$Nu_x = \frac{\text{convective heat transfer coefficient}}{\text{conductive heat transfer coefficient}} \quad (1.15)$$

Now heat transfer by convection is $(h\Delta T)$ and by conduction is $(k\Delta T/x)$. So Nusselt number becomes

$$Nu_x = \frac{h\Delta T}{k\Delta T/x} = \frac{hx}{k} \quad (1.16)$$

Here h is the convective heat transfer, x is the characteristic length and k is the thermal conductivity of the fluid.

1.14.6 Skin friction

When fluid transfers through a surface certain amount of friction acts known as skin friction. It arises between the fluid and the surface, which tends to stress-free the fluid's motion. The skin friction coefficient mathematically written as

$$C_f = \frac{\tau_w}{\rho U^2/2} \quad (1.17)$$

where τ_w is the shear stress at the wall, ρ is the density and U is free-stream velocity.

1.14.7 Sherwood number

It is a dimensionless number, denoted with Sh_x , and is used in mass-transfer operation. It also known as mass transfer Nusselt number. Sherwood number represents the ratio of convective to diffusive mass transport. It was proposed by Thomas Kilgore Sherwood. The mathematical form of Sherwood number is listed below,

$$Sh_x = \frac{\text{Convective mass transfer coefficient}}{\text{Diffusive mass transfer coefficient}} \quad (1.18)$$

representing the mass transfer by convection with β and mass transfer by diffusion with δ/x , we write it as,

$$Sh_x = \frac{\beta}{D/x} = \frac{\beta x}{D}. \quad (1.19)$$

Here β is the mass transfer coefficient with unit (m/s) , x is a characteristic length with unit (m) and D is mass diffusivity with unit (m^2/s) .

1.15 Some basic equations

1.15.1 Continuity equation

Continuity equation is derived from the law of conservation of mass. Mathematically it can be written as

$$\frac{\partial \rho}{\partial t} + \nabla \cdot (\rho \mathbf{V}) = 0, \quad (1.20)$$

here ρ is fluid density, \mathbf{V} the velocity field and t is the time. If the fluid is an incompressible then the continuity equation for such fluids can be obtained as

$$\nabla \cdot \mathbf{V} = 0. \quad (1.21)$$

1.15.2 Equation of motion

The conservation law of momentum state that

$$\rho \frac{d\mathbf{V}}{dt} = \text{div } \boldsymbol{\tau} + \mathbf{b}, \quad (1.22)$$

here $\boldsymbol{\tau}$ is Cauchy stress tensor that is different for different fluid, \mathbf{b} denotes the body force and d/dt represents the material derivative, defined by

$$\frac{d}{dt} = \frac{\partial}{\partial t} + (\nabla \cdot \mathbf{V}). \quad (1.23)$$

1.15.3 Energy equation

The thermal energy equation for nanofluid with viscous dissipation effects can be expressed as

$$(\rho C_p)_f \left(\frac{\partial}{\partial t} + \mathbf{V} \cdot \nabla \right) T = k \nabla^2 T + \boldsymbol{\tau} \cdot \mathbf{L} + (\rho C_p)_s \left[D_B \nabla \cdot C \cdot \nabla T + \frac{D_T}{T_m} \nabla T \cdot \nabla T \right], \quad (1.24)$$

where $(C_p)_f$ represents the specific heat of base fluid, $(C_p)_s$ denotes the specific heat of material, ρ_f the density of base fluid, ρ_s the density of nanoparticles, k the thermal conductivity, \mathbf{L} denotes the rate of strain tensor and T is the temperature of the fluid. D_B represents the Brownian motion coefficient, D_T denotes the Thermophoretic diffusion coefficient and T_m is the mean temperature.

The expression for Cauchy stress tensor $\boldsymbol{\tau}$ for viscous incompressible fluid can be write down as

$$\boldsymbol{\tau} = -P\mathbf{I} + \mu\mathbf{A}_1, \quad (1.25)$$

here p denotes the pressure, \mathbf{I} is the identity tensor, μ denotes the dynamic viscosity of the fluid and the first Rivlin-Ericksen tensor were represented with \mathbf{A}_1 that is given by

$$\mathbf{A}_1 = (\text{grad } \mathbf{V}) + (\text{grad } \mathbf{V})^\star, \quad (1.26)$$

the \star in superscript is the representation of the matrix transpose. For two dimensional velocity field, the strain tensor can be defined as

$$\mathbf{L} = \text{grad } \mathbf{V} = \begin{bmatrix} u_x & u_y & 0 \\ v_x & v_y & 0 \\ 0 & 0 & 0 \end{bmatrix}. \quad (1.27)$$

Substituting Eqs.(1.26) and (1.27) in Eq. (1.25) we get

$$\boldsymbol{\tau} = \begin{bmatrix} -p + 2\mu u_x & \mu(u_y + v_x) & 0 \\ \mu(u_x + v_y) & -p + 2\mu v_y & 0 \\ 0 & 0 & 0 \end{bmatrix} \quad (1.28)$$

also

$$\boldsymbol{\tau} \cdot \mathbf{L} = \text{tr}(\boldsymbol{\tau} \mathbf{L}) = \tau_{xx} + \tau_{xy}(u_y + v_x) + \tau_{yy}. \quad (1.29)$$

1.15.4 Concentration equation

The concentration equation for nanofluid can be defined as

$$\left(\frac{\partial}{\partial t} + \mathbf{V} \cdot \nabla\right) C = D_B \nabla^2 C + \frac{D_T}{T_m} \nabla^2 T, \quad (1.30)$$

here C is the concentration of nanoparticles, D_B represents the Brownian motion coefficient, D_T denotes the coefficient of diffusivity and T_m is the mean temperature.

1.16 Homotopy analysis method

We have solved the non-linear problems through homotopy analysis method (HAM), Suggested by Liao [22]. For the elementary idea of homotopy analysis method, we study the following differential equation

$$N[\xi(x)] = 0, \quad (1.31)$$

where N is a non-linear operator, x is the independent variable and $\xi(x)$ is the unknown function. The zeroth-order deformation equation is

$$(1-p)\mathcal{L}[\widehat{\xi}(x;p) - u_0(x)] = p\hbar N[\widehat{\xi}(x;p)], \quad (1.32)$$

in which $\xi_0(x)$ indicates the initial approximation, \mathcal{L} is the auxiliary linear operator, $p \in [0, 1]$ is an embedding parameter, \hbar is an auxiliary parameter and $\widehat{\xi}(x;p)$ is unknown function of x and p .

For $p = 0$ and $p = 1$, One has

$$\widehat{\xi}(x;0) = \xi_0(x), \quad \text{and} \quad \widehat{\xi}(x;1) = \xi(x) \quad (1.33)$$

As when p varies from 0 to 1, the solution $\widehat{\xi}(x;p)$ varies from initial approximation $\xi_0(x)$ to

the final solution $\xi(x)$. By Taylor series expansion one can write

$$\widehat{\xi}(x;p) = \xi_0(x) + \sum_{m=1}^{\infty} \xi_m(x) p^m, \quad \xi_m(x) = \frac{1}{m!} \left. \frac{\partial^m \widehat{\xi}(x;p)}{\partial p^m} \right|_{p=0}. \quad (1.34)$$

when $p = 1$, we get

$$\xi(x) = \xi_0(x) + \sum_{m=1}^{\infty} \xi_m(x) \quad (1.35)$$

To obtain m -th order deformation equation, differentiating m -time Eq. (1.28) with respect to p , dividing both sides by $m!$ and finally substituting $p = 0$, we get

$$\mathcal{L} [\xi_m(x) - \chi_m \xi_{m-1}(x)] = \hbar \mathcal{R}_m(x), \quad (1.36)$$

$$\mathcal{R}_m(x) = \frac{1}{(m-1)!} \left. \frac{\partial^m N[\widehat{\xi}(x;p)]}{\partial p^m} \right|_{p=0} \quad (1.37)$$

with

$$\chi_m = \begin{cases} 0, & m \leq 1 \\ 1, & m > 1 \end{cases}. \quad (1.38)$$

Chapter 2

Natural convection along a vertical isothermal plate with linear and non-linear Rosseland thermal radiation

2.1 Introduction

Here we have studied the steady laminar natural convection flow along a vertical isothermal plate with linear or non-linear Rosseland radiation. The parameters involve in the problem are Prandtl number, temperature parameter, radiation parameter, and the effects of the present parameters on the results are accessible in tables and figures. Here the radiation parameter is defined with a new and different way. From tables, it is exposed that once the wall shear stress rises the wall heat transfer reduces and vice versa. Here the nonlinear partial differential equations of this work are transformed to the ordinary differential equations by appropriate similarity transformations. Homotopy analysis method (HAM) has been used for the solution of the problem. we have also checked the convergence of problem. The effects of certain parameters can be understood through graphs and tabulated values. The numerical values are computed and analyzed for local Nusselt number and skin friction coefficient. The work in this

chapter is a review of research paper [12].

2.2 Mathematical formulation

Here the fluid flow along a vertical, semi-infinite plate. The velocity components in the x and y directions are denoted with u and v respectively, Cartesian coordinates (x, y) are used in which plate lies on x coordinate where as y is perpendicular to x . The boundary layer equations for two-dimensional, steady fluid flow are

$$\nabla \cdot \mathbf{V} = 0, \quad (2.1)$$

$$\rho \frac{d\mathbf{V}}{dt} = \text{div} \cdot \boldsymbol{\tau} + \rho \mathbf{b}, \quad (2.2)$$

The velocity field for the present flow is

$$\mathbf{V} = [u(x, y), v(x, y), 0]. \quad (2.3)$$

By invoking velocity field (2.3) and Cauchy stress tensor for viscous fluid defined by (1.25), the boundary layer equation in the presence of buoyance forces becomes

$$u \frac{\partial u}{\partial x} + v \frac{\partial u}{\partial y} = -\frac{1}{\rho} \frac{\partial P}{\partial x} + \nu \frac{\partial^2 u}{\partial y^2} + g\beta_T (T - T_\infty). \quad (2.4)$$

In the above expressions u and v are the velocity components in the x and y -direction, ρ is the density, P is the pressure, β_T is the thermal expansion coefficient and ν is kinematic viscosity.

The energy equation for the present problem is

$$\rho c_p \frac{dT}{dt} = \boldsymbol{\tau} \cdot \mathbf{L} - \text{div} \mathbf{q}, \quad (2.5)$$

$$\mathbf{q} = -k_1 \text{grad} T, \quad (2.6)$$

where ρ is the density of fluid, c_p is the specific heat, $\boldsymbol{\tau}$ is the Cauchy stress tensor, \mathbf{L} is the velocity gradient, T is the temperature, \mathbf{q} is the heat flux, q_r is the radiation heat flux and k_1 is the fluid thermal conductivity. Eq. (2.5) in the absence of viscous dissipation and in the

presence of Rosseland approximations becomes

$$\left(u \frac{\partial T}{\partial x} + v \frac{\partial T}{\partial y} \right) = \frac{k_1}{\rho c_p} \frac{\partial^2 T}{\partial y^2} - \frac{1}{\rho c_p} \frac{\partial q_r}{\partial y}. \quad (2.7)$$

The subjected boundary conditions are

$$\begin{aligned} u &= 0, & v &= 0, & T &= T_w & \text{at } y &= 0, \\ u &\rightarrow 0, & v &\rightarrow 0 & T &\rightarrow T_\infty & \text{as } y &\rightarrow \infty. \end{aligned} \quad (2.8)$$

The Rosseland [24] approximation of radiation for an optically thick media and gives the net radiation heat flux

$$q_r = -\frac{4}{3\alpha_R} \text{grad}(e_b), \quad (2.9)$$

where $\alpha_R [m^{-1}]$ is the Rosseland mean absorption coefficient and $e_b [Wm^{-2}]$ is the blackbody emissive power that is assumed in terms of the absolute temperature T by the Stefan-Boltzmann radiation law, $e_b = \sigma_{SB} T^4$, with the Stefan-Boltzmann constant $\sigma_{SB} = 5.6697 \times 10^{-8} Wm^{-2} K^{-4}$.

For a plane boundary layer flow over a hot surface, Eq. (2.9) of the net radiation heat flux absorbed in the fluid is reduces to

$$q_r = -\frac{16\sigma_{SB}}{3\alpha_R} T^3 \frac{dT}{dy}, \quad (2.10)$$

Here T^4 is stated as a linear function of temperature by using Taylor series expansion about T_∞ is

$$T^4 = 4T_\infty^3 T - 3T_\infty^4. \quad (2.11)$$

Introducing the following similarity transformations [25],

$$\begin{aligned} \psi &= 2x^{\frac{3}{4}} [g\beta(T_w - T_\infty)]^{\frac{1}{4}} \sqrt{2\nu} f(\eta), \quad \theta = \frac{T - T_\infty}{T - T_w}, \quad \theta_w = \frac{T_w + T_\infty}{2}, \\ \text{Re} &= \frac{[g\beta(T_w - T_\infty)]^{\frac{1}{2}} x^2}{\nu}, \quad \eta = \frac{y}{x} \left[\frac{Gr}{4} \right]^{\frac{1}{4}}, \quad Gr = \frac{g\beta(T_w - T_\infty) x^3}{\nu^2}, \end{aligned} \quad (2.12)$$

$$v = \frac{y [g\beta (T_w - T_\infty)]^{\frac{1}{2}}}{2\sqrt{x}} f'(\eta) - \frac{3 [g\beta (T_w - T_\infty)]^{\frac{1}{4}} \nu^{\frac{1}{2}}}{\sqrt{2}x^{\frac{1}{4}}} f(\eta), \quad u = 2 [g\beta (T_w - T_\infty)]^{\frac{1}{2}} x^{\frac{1}{2}} f'(\eta). \quad (2.13)$$

Using Eqs. (2.12) and (2.13) into Eqs. (2.1), (2.4), (2.7) and (2.8), it is noted that Eq. (2.1) is identically satisfied while rest of the equations are transformed into following system of nonlinear equations.

$$\begin{aligned} f''' + 3ff'' - 2f'^2 + \theta &= 0, \\ (1 + Rd\theta_w^3) \theta'' + 3Pr f\theta' &= 0, \end{aligned} \quad (2.14)$$

$$\begin{aligned} f &= f' = 0, \quad \theta = 1, \quad \text{at } \eta = 0, \\ f' &= 0, \quad \theta \rightarrow 0 \quad \text{as } \eta \rightarrow \infty, \end{aligned} \quad (2.15)$$

where

$$Rd = \frac{16\sigma_{SB}T_\infty^3}{3k\alpha_R}, \theta_w = \frac{T_w}{T_\infty}, Pr = \frac{\nu}{\alpha}. \quad (2.16)$$

The skin friction coefficient and the local Nusselt number are defined as

$$C_f = \frac{\tau_{xy}(0)}{\rho U^2/2}, \quad \text{and} \quad Nu_x = \frac{xq_w}{k_0(T - T_\infty)}, \quad (2.17)$$

with

$$\tau_{xy} = \mu \left(\frac{\partial u}{\partial y} \right)_{y=0}, \quad q_w = -k_0 \left. \frac{\partial T}{\partial y} \right|_{y=0} + q_r|_{y=0}. \quad (2.18)$$

Using similarity transformations in Eqs. (2.17) and (2.18) we get

$$\frac{1}{\sqrt{2}\nu} x^{\frac{5}{4}} f'(\eta) Re^{-\frac{1}{2}} C_f = f''(0), \quad \sqrt{2}x^{\frac{1}{4}} Nu_x Re^{-\frac{1}{2}} = -(1 + Rd\theta_w^3) \theta'(0). \quad (2.19)$$

2.3 Solutions by the homotopy analysis method

As we know that the homotopy solutions depend on the initial guesses (f_0, θ_0) and auxiliary linear operators (L_f, L_θ) which are chosen in the forms

$$f_0 = 0, \quad \theta_0 = \text{Exp}(-\eta), \quad (2.20)$$

$$\mathcal{L}_f [f(\eta)] = \frac{\partial^3 f}{\partial \eta^3} - \frac{\partial f}{\partial \eta}, \quad \mathcal{L}_\theta [\theta(\eta)] = \frac{\partial^2 \theta}{\partial \eta^2} - \theta, \quad (2.21)$$

with the properties

$$\begin{aligned} \mathcal{L}_f [C_1 e^{-\eta} + C_2 e^\eta + C_3] &= 0, \\ \mathcal{L}_\theta [C_4 e^{-\eta} + C_5 e^\eta] &= 0, \end{aligned} \quad (2.22)$$

where C_i ($i = 1 - 5$) are the arbitrary constants.

2.3.1 Zeroth order problem

$$\begin{aligned} (1-p) \mathcal{L}_f [\hat{f}(\eta; p) - f_0(\eta)] &= p \hbar_f \mathcal{N}_f [\hat{f}(\eta; p)], \\ (1-p) \mathcal{L}_\theta [\theta(\eta; p) - \theta_0(\eta)] &= p \hbar_\theta \mathcal{N}_\theta [\theta(\eta; p)], \end{aligned} \quad (2.23)$$

$$\begin{aligned} \hat{f}(0; p) &= \frac{\partial \hat{f}(0; p)}{\partial \eta} = 0, \quad \theta(0; p) = 1, \quad \text{as } \eta = 0, \\ \frac{\partial \hat{f}(\eta)}{\partial \eta} &= 1, \quad \theta(\eta) \rightarrow 0 \quad \text{as } \eta \rightarrow \infty, \end{aligned} \quad (2.24)$$

where \hbar_f and \hbar_θ are the non-zero auxiliary parameters, $p \in [0, 1]$ is the embedding parameter and the nonlinear operators \mathcal{N}_f and \mathcal{N}_θ are

$$\mathcal{N}_f [\hat{f}(\eta, p)] = \frac{\partial^3 \hat{f}}{\partial \eta^3} + 3\hat{f} \frac{\partial^2 \hat{f}}{\partial \eta^2} - 2 \left(\frac{\partial \hat{f}}{\partial \eta} \right)^2 + \theta, \quad (2.25)$$

$$\mathcal{N}_\theta [\theta(\eta; q)] = (1 + R d \theta_w^3) \frac{\partial^2 \theta}{\partial \eta^2} + 3 \text{Pr} f \frac{\partial \theta}{\partial \eta}, \quad (2.26)$$

$$\widehat{f}(\eta, 0) = f_0(\eta), \quad \widehat{\theta}(\eta, 0) = \theta_0(\eta), \quad (2.27)$$

$$\widehat{f}(\eta, 1) = f(\eta), \quad \widehat{\theta}(\eta, 1) = \theta(\eta), \quad (2.28)$$

when p varies from 0 to 1 then $\widehat{f}(\eta, p)$ and $\widehat{\theta}(\eta, p)$ vary from the initial guesses $f_0(\eta)$ and $\theta_0(\eta)$ to the final solutions $f(\eta)$ and $\theta(\eta)$ respectively. Expanding $\widehat{f}(\eta, p)$ and $\widehat{\theta}(\eta, p)$ in Taylor's series with respect to the embedding parameter p one can write

$$\widehat{f}(\eta, p) = f_0(\eta) + \sum_{k=1}^{\infty} f_k(\eta) p^k, \quad f_k(\eta) = \left. \frac{1}{k!} \frac{\partial^k \widehat{f}(\eta, p)}{\partial p^k} \right|_{p=0}, \quad (2.29)$$

$$\widehat{\theta}(\eta, p) = \theta_0(\eta) + \sum_{k=1}^{\infty} \theta_k(\eta) p^k, \quad \theta_k(\eta) = \left. \frac{1}{k!} \frac{\partial^k \widehat{\theta}(\eta, p)}{\partial p^k} \right|_{p=0}. \quad (2.30)$$

The auxiliary parameters \hbar_f and \hbar_θ are suitably chosen that the series (2.29) and (2.30) converge at $p = 1$. Hence we have

$$f(\eta) = f_0(\eta) + \sum_{k=1}^{\infty} f_k(\eta), \quad (2.31)$$

$$\theta(\eta) = \theta_0(\eta) + \sum_{k=1}^{\infty} \theta_k(\eta). \quad (2.32)$$

2.3.2 k th-order deformation problems

Differentiating the zeroth-order deformation problem (2.23) k -times with respect to p , dividing by $k!$ and setting $p = 0$, the k th-order deformation problem is given by

$$\begin{aligned} \mathcal{L}_f [f_k(\eta) - \chi_k f_{k-1}(\eta)] &= \hbar_f \mathcal{R}_{f,k}(\eta), \\ \mathcal{L}_\theta [\theta_k(\eta) - \chi_k \theta_{k-1}(\eta)] &= \hbar_\theta \mathcal{R}_{\theta,k}(\eta), \end{aligned} \quad (2.33)$$

$$\begin{aligned} f_k(0) &= 0, & f'_k(0) &= 0, & \theta_k(0) &= 0, \\ f'_k(\eta) &= 0, & \theta_k(\eta) &= 0, & \text{as } \eta &\rightarrow \infty. \end{aligned} \quad (2.34)$$

With the results stated below,

$$\begin{aligned}\mathcal{R}_k^f(\eta) &= \frac{\partial^3 f_{k-i-1}}{\partial \eta^3} + 3 \sum_{i=0}^{k-1} f_i \frac{\partial^2 f_{k-i-1}}{\partial \eta^2} - 2 \sum_{i=0}^{k-1} \frac{\partial f_i}{\partial \eta} \frac{\partial f_{k-i-1}}{\partial \eta} + \theta_{k-1}, \\ \mathcal{R}_k^\theta(\eta) &= (1 + Rd\theta_w^3) \frac{\partial^2 \theta_{k-1}}{\partial \eta^2} + 3Pr \sum_{i=0}^{k-1} f_i \frac{\partial \theta_{k-i-1}}{\partial \eta}.\end{aligned}\quad (2.35)$$

where

$$\chi_k = \begin{cases} 0, & k \leq 1 \\ 1, & k > 1 \end{cases}.\quad (2.36)$$

The general solutions of the system (2.35) can be written as

$$f_k(\eta) = f_k^*(\eta) + A_1 + A_2 e^\eta + A_3 e^{-\eta},\quad (2.37)$$

$$\theta_k(\eta) = \theta_k^*(\eta) + A_4 e^\eta + A_5 e^{-\eta},\quad (2.38)$$

in which f_k^* and θ_k^* are the special solutions and the values of A_i ($i = 1 - 5$) after using the boundary conditions (2.37) and (2.38) are given by

$$A_1, A_2, A_3 = 0 = A_4, A_5 = \theta_k^*(\eta)|_{\eta=0},\quad (2.39)$$

Note that the solutions of the problems involving Eqs. (2.35) – (2.39) are constructed using the symbolic computation software MATHEMATICA when $k = 1, 2, 3, \dots$

2.4 Analysis of the solutions

2.4.1 Convergence of the series solution

We know that the series solutions contain auxiliary parameters \hbar_f and \hbar_θ . The convergence of series solutions depend upon these parameters. The relevant \hbar -curves have been sketched in the Figs. 2.1 and 2.2. It is noticed that the admissible ranges of \hbar_f and \hbar_θ are $-1.5 \leq \hbar_f \leq -0.5$

and $-1.6 \leq \tilde{h}_\theta \leq -0.4$.

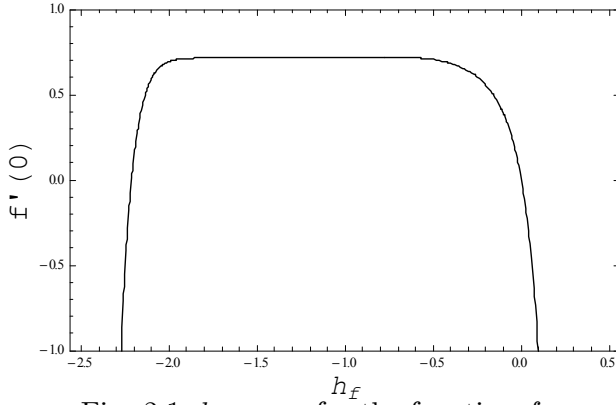


Fig. 2.1. h -curve for the function f .

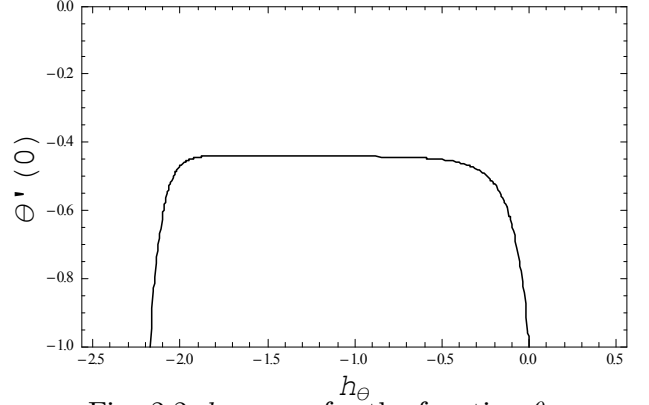


Fig. 2.2. h -curve for the function θ .

2.4.2 Discussion

Here we study the consequences of distinct embedded parameters on the velocity and temperature profiles. Accordingly, Figs. 2.3 – 2.8 have been constructed. Figs. 2.3 show the effect of Pr on the velocity profile. It is perceived that increasing the Pr the velocity profile decreases. The velocity boundary layer thickness decreases with an increase in Pr . On the other hand, it gives opposite behavior for θ , which can be seen in the Figs. 2.6. This Fig. shows that due to the increase in Pr number the velocity profile increases. The influence of radiation parameter Rd are shown in Fig. 2.4 and 2.7. The effects of Rd on velocity profile is constructed in Figs. 2.4. It is noticed increasing the values of Rd , both the velocity as well as the temperature profile increases, as shown in Figs. 2.4 and 2.7. Further the behaviors of the temperature parameter θ_w on velocity and temperature profiles are shown in Figs. 2.5 and 2.8. The velocity as well as the temperature profiles are increasing with increase in the temperature parameter θ_w .

Table 2 shows the effects of $f''(0)$ and $(-\theta'(0))$ for different values of parameters. The magnitude of skin friction coefficient increases with the increase in θ_w and Rd while decreases with increase in Pr . On the other hand the magnitude of local Nusselt number increases with

the increase in Pr , and decreases with an increase in θ_w and Rd .

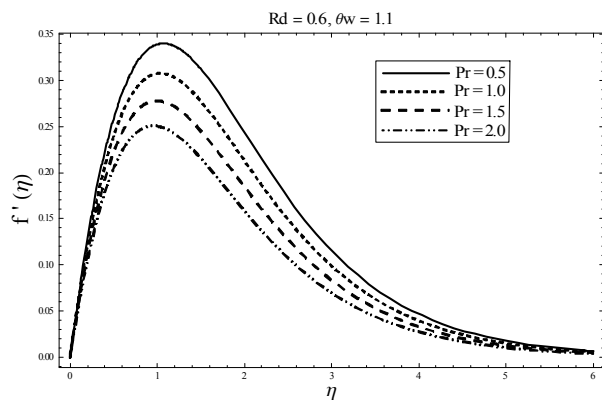


Fig. 2.3. Effects of Pr on $f'(\eta)$.

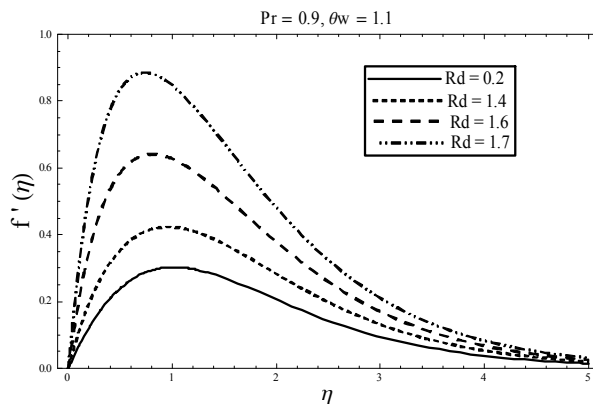


Fig. 2.4. Effects of Rd on $f'(\eta)$.

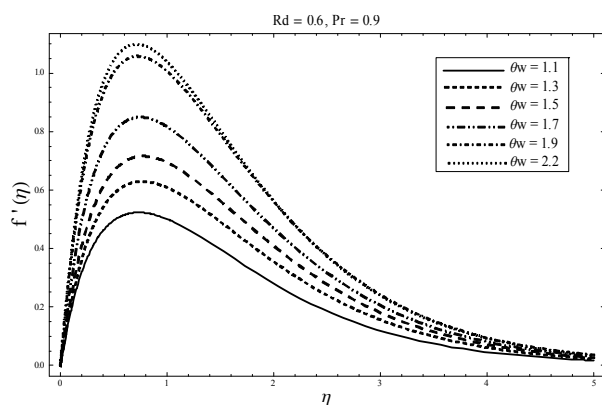


Fig. 2.5. Effects of θ_w on $f'(\eta)$.

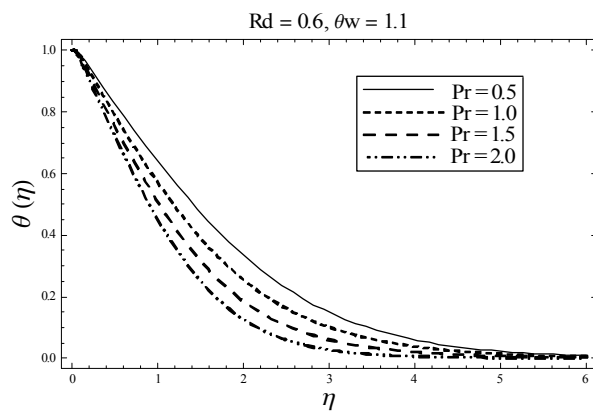


Fig. 2.6. Effects of Pr on $\theta(\eta)$.

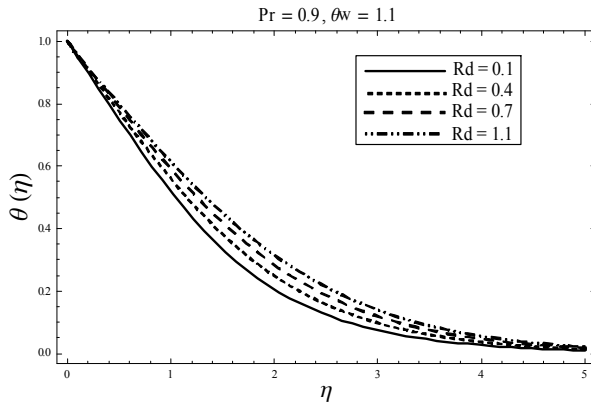


Fig. 2.7. Effects of Rd on $\theta(\eta)$.

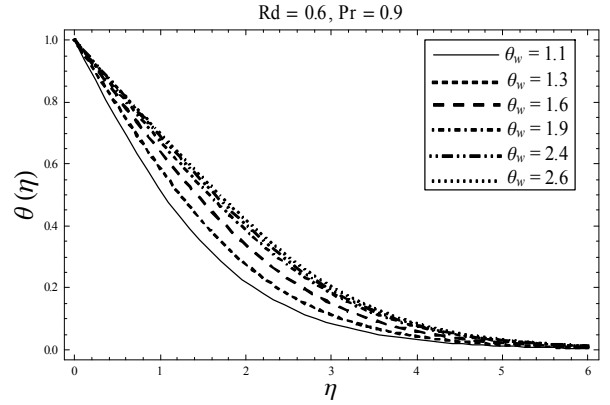


Fig. 2.8. Effects of θ_w on $\theta(\eta)$.

Table. 2.2. Skin friction $(1 + Rd) f''(0)$ and local Nusselt number $-\theta'(0)$ for different values of the parameters

θ_w	$Rd = 0.6$		$Rd = 0.7$		$Rd = 0.9$	
	$(1 + Rd) f''(0)$	$-\theta'(0)$	$(1 + Rd) f''(0)$	$-\theta'(0)$	$(1 + Rd) f''(0)$	$-\theta'(0)$
Pr = 0.8						
1.1	0.7245	0.6766	0.7311	0.6999	0.7409	0.7523
1.2	0.7357	0.6457	0.7414	0.6689	0.7560	0.7038
1.3	0.7450	0.6230	0.7548	0.6325	0.7676	0.6671
Pr = 0.9						
1.1	0.7145	0.7053	0.7208	0.7301	0.7322	0.7785
1.2	0.7252	0.6746	0.7322	0.6969	0.7454	0.7363
1.3	0.7361	0.6440	0.7448	0.6601	0.7558	0.7066
Pr = 1.0						
1.1	0.7048	0.7338	0.7114	0.7591	0.7230	0.8092
1.2	0.7158	0.7007	0.7233	0.7226	0.7356	0.7656
1.3	0.7274	0.6687	0.7357	1.0247	0.7498	0.7227

2.5 Concluding Remarks

The effect of either linear or non-linear Rosseland radiation on the natural convection along a vertical isothermal plate has been explore in this work. Finally we have computed the series solutions by the homotopy analysis method (HAM). The main theme of the present analysis are as follows.

- ▶ The velocity and temperature profile decreases with the increase of Pr number.
- ▶ The velocity and temperature profile increases with the increase of Rd parameter.
- ▶ With the increase in temperature parameter θ_w , the velocity and temperature profiles increases, and for higher values of θ_w , the temperature and the velocity profiles goes to an asymptotic state.

Chapter 3

MHD Flow of a Second Grade Nanofluid with Thermal radiation

3.1 Introduction

This chapter consists of the series solution for Rosseland thermal radiation and mixed convection fluid flow of an incompressible fluid. Squeezing flow of a second grade fluid between two parallel plates is considered. The upper plate is taken to be impermeable but capable of moving towards or away from the lower fixed plate. The squeezing is a fundamental type of flow that is commonly seemed in multiple hydro dynamic tools and machines. A combination of base fluid and nanoparticle is new variability of energy transport fluids recognized as nanofluid. Governing equations are obtained with the help of conservation laws mutual with suitable similarity transformations. Homotopy analysis method (HAM) and Optimal homotopy analysis method (OHAM) is then utilized to find the solutions of coupled nonlinear ordinary differential equation. Special effects of various physical parameters on the flow are also deliberated with the support of graphs along with broad discussion.

3.2 Mathematical model

Consider the second grade two-dimensional flow of nanofluid stuck between plates separated by a distance $h(t) = \sqrt{\frac{v(1-\gamma t)}{a}}$. The lower plate is stretching in an unsteady way with the velocity

$\frac{ax}{(1-\gamma t)}$ for $(t < \frac{1}{\gamma})$. Keep in mind that for $\gamma = 0$, the steady state situation is recovered. Here the strength H of magnetic field is applied in the y -direction whereas the induced magnetic field is ignored subject to the small magnetic Reynolds number. Heat transfer analysis is allowed in the presence of nonlinear thermal radiations. The plate is sustained at constant temperature T_w where as T_0 is the ambient fluid's temperature. The governing equations of motion, energy and nanoparticles are stated as

$$\nabla \cdot \mathbf{V} = 0, \quad (3.1)$$

$$\rho \frac{d\mathbf{V}}{dt} = \nabla \cdot \boldsymbol{\tau} + \rho g \beta_T (T - T_\infty) + \rho g \beta_C (C - C_0) + \mathbf{J} \times \mathbf{B}, \quad (3.2)$$

$$\rho c_p \frac{dT}{dt} = \mathbf{T} \cdot \mathbf{L} - \text{div } \mathbf{q}, \quad (3.3)$$

$$\left(\frac{\partial}{\partial t} + \mathbf{V} \cdot \nabla \right) C = D_B \nabla^2 C + \frac{D_T}{T_m} \nabla^2 T, \quad (3.4)$$

the Cauchy stress tensor for a second grade fluid is defined as

$$\boldsymbol{\tau} = -p\mathbf{I} + \mu \mathbf{A}_1 + \alpha_1 \mathbf{A}_1 + \alpha_1 \mathbf{A}_2 + \alpha_2 \mathbf{A}_1^2, \quad (3.5)$$

$$\mathbf{A}_1 = (\text{grad } \mathbf{V}) + (\text{grad } \mathbf{V})^\star \quad (3.6)$$

$$\mathbf{A}_2 = \frac{d\mathbf{A}_1}{dt} + \mathbf{A}_1 (\text{grad } \mathbf{V}) + (\text{grad } \mathbf{V})^\star \mathbf{A}_1,$$

$$\begin{aligned} \mathbf{J} &= \sigma (\mathbf{V} \times \mathbf{B}) \\ \mathbf{q} &= -k \text{grad } T, \end{aligned} \quad (3.7)$$

and the velocity field is

$$\mathbf{V} = [u(x, y, t), v(x, y, t), 0]. \quad (3.8)$$

In the above expressions \mathbf{V} is the velocity, $\boldsymbol{\tau}$ is the Cauchy stress tensor, p is the pressure, g is the gravitational acceleration which acts in the downward direction, α_j ($j = 1, 2$) the material constants, here \star in the superscript denotes the transpose of matrix, ρ is the density of the fluid, c_p is the specific heat at constant pressure, \mathbf{L} is the gradient of velocity, $\frac{d}{dt}$ is the covariant derivative, μ is the dynamic viscosity, $\mathbf{A}_1, \mathbf{A}_2$ both are the first Rivlin-Ericksen tensor, \mathbf{q} is the

heat flux, k is the thermal conductivity, σ is the electrical conductivity, \mathbf{B} is the magnetic field, T is the temperature and C is the concentration of nanoparticles, D_B represents the Brownian motion coefficient, D_T denotes the coefficient of diffusivity and T_m is the mean temperature. Keep in mind that the Clausius–Duhem inequality is holed and Helmholtz free energy is minimum in equilibrium for the fluid locally at rest when

$$\mu \geq 0, \quad \alpha_1 \geq 0, \quad \alpha_1 + \alpha_2 = 0.$$

Here first Rivlin–Ericksen tensor is

$$\mathbf{A}_1 = \begin{bmatrix} 2\frac{\partial u}{\partial x} & \frac{\partial u}{\partial y} + \frac{\partial v}{\partial x} & 0 \\ \frac{\partial u}{\partial y} + \frac{\partial v}{\partial x} & 2\frac{\partial v}{\partial y} & 0 \\ 0 & 0 & 0 \end{bmatrix}. \quad (3.9)$$

$$\mathbf{A}_2 = \begin{bmatrix} 2 \left(\frac{\partial^2 u}{\partial t \partial x} + u \frac{\partial^2 u}{\partial x^2} + v \frac{\partial^2 u}{\partial y \partial x} + 2 \left(\frac{\partial u}{\partial x} \right)^2 + \frac{\partial v}{\partial x} \left(\frac{\partial u}{\partial y} + \frac{\partial v}{\partial x} \right) \right) & \frac{\partial^2 u}{\partial t \partial y} + \frac{\partial^2 v}{\partial t \partial y} + u \left(\frac{\partial^2 u}{\partial y \partial x} + \frac{\partial^2 v}{\partial x^2} \right) + v \left(\frac{\partial^2 u}{\partial y^2} + \frac{\partial^2 v}{\partial y \partial x} \right) + 2 \frac{\partial u}{\partial x} \frac{\partial u}{\partial y} + \frac{\partial v}{\partial y} \left(\frac{\partial u}{\partial y} + \frac{\partial v}{\partial x} \right) + \frac{\partial u}{\partial x} \left(\frac{\partial u}{\partial y} + \frac{\partial v}{\partial x} \right) + 2 \frac{\partial v}{\partial x} \frac{\partial v}{\partial y} & 0 \\ \frac{\partial^2 u}{\partial t \partial y} + \frac{\partial^2 v}{\partial t \partial y} + u \left(\frac{\partial^2 u}{\partial y \partial x} + \frac{\partial^2 v}{\partial x^2} \right) + v \left(\frac{\partial^2 u}{\partial y^2} + \frac{\partial^2 v}{\partial y \partial x} \right) + 2 \frac{\partial u}{\partial x} \frac{\partial u}{\partial y} + \frac{\partial v}{\partial y} \left(\frac{\partial u}{\partial y} + \frac{\partial v}{\partial x} \right) + \frac{\partial u}{\partial x} \left(\frac{\partial u}{\partial y} + \frac{\partial v}{\partial x} \right) + 2 \frac{\partial v}{\partial x} \frac{\partial v}{\partial y} & 2 \left(\frac{\partial^2 v}{\partial t \partial y} + v \frac{\partial^2 v}{\partial y^2} + u \frac{\partial^2 v}{\partial y \partial x} + 2 \left(\frac{\partial v}{\partial y} \right)^2 + \frac{\partial u}{\partial y} \left(\frac{\partial u}{\partial y} + \frac{\partial v}{\partial x} \right) \right) & 0 \\ 0 & 0 & 0 \end{bmatrix} \quad (3.10)$$

Using the above information we get,

$$\begin{aligned} \frac{\partial u}{\partial t} + u \frac{\partial u}{\partial x} + v \frac{\partial u}{\partial y} &= -\frac{1}{\rho_f} \frac{\partial p}{\partial x} + v \left(\frac{\partial^2 u}{\partial x^2} + \frac{\partial^2 u}{\partial y^2} \right) + \frac{\alpha_1}{\rho} \left[\begin{aligned} &\frac{\partial^3 u}{\partial t \partial x^2} + \frac{\partial^3 u}{\partial t \partial y^2} + 2 \frac{\partial v}{\partial y} \frac{\partial^2 v}{\partial x \partial y} \\ &+ u \left(\frac{\partial^3 u}{\partial x^3} + \frac{\partial^3 u}{\partial x \partial y^2} \right) + v \left(\frac{\partial^3 u}{\partial x^2 \partial y} + \frac{\partial^3 u}{\partial y^3} \right) \\ &+ \frac{\partial u}{\partial x} \left(3 \frac{\partial^2 u}{\partial x^2} + \frac{\partial^2 u}{\partial y^2} \right) + \frac{\partial u}{\partial y} \left(\frac{\partial^2 u}{\partial x \partial y} + \frac{\partial^2 v}{\partial x^2} \right) \end{aligned} \right] \\ &- \frac{\sigma_m H^2(t)}{\rho(1-\gamma t)} u + g\beta_T(T - T_0) + g\beta_C(C - C_0), \end{aligned} \quad (3.11)$$

$$\frac{\partial v}{\partial t} + u \frac{\partial v}{\partial x} + v \frac{\partial v}{\partial y} = -\frac{1}{\rho_f} \frac{\partial p}{\partial y} + \nu \left(\frac{\partial^2 v}{\partial x^2} + \frac{\partial^2 v}{\partial y^2} \right) + \frac{\alpha_1}{\rho} \left[\begin{aligned} & \frac{\partial^3 v}{\partial t \partial x^2} + \frac{\partial^3 v}{\partial t \partial y^2} + 2 \frac{\partial u}{\partial y} \frac{\partial^2 v}{\partial y^2} + u \left(\frac{\partial^3 v}{\partial x^3} + \frac{\partial^3 v}{\partial x \partial y^2} \right) + \\ & v \left(\frac{\partial^3 v}{\partial y^3} + \frac{\partial^3 v}{\partial x^2 \partial y} \right) + \frac{\partial v}{\partial x} \left(\frac{\partial^2 u}{\partial y^2} + \frac{\partial^2 v}{\partial x \partial y} \right) + \frac{\partial v}{\partial y} \left(\frac{\partial^2 v}{\partial x^2} + 3 \frac{\partial^2 v}{\partial y^2} \right) \end{aligned} \right], \quad (3.12)$$

$$\begin{aligned} \frac{\partial T}{\partial t} + u \frac{\partial T}{\partial x} + v \frac{\partial T}{\partial y} &= \alpha_f \left(\frac{\partial^2 T}{\partial x^2} + \frac{\partial^2 T}{\partial y^2} \right) + \tau \left\{ D_B \left(\frac{\partial C}{\partial x} \frac{\partial T}{\partial x} + \frac{\partial C}{\partial y} \frac{\partial T}{\partial y} \right) \right. \\ &\quad \left. + \left(\frac{D_T}{T_0} \right) \left[\left(\frac{\partial T}{\partial x} \right)^2 + \left(\frac{\partial T}{\partial y} \right)^2 \right] \right\} - \frac{1}{(\rho c_p)_f} \frac{\partial q_r}{\partial y}, \end{aligned} \quad (3.13)$$

$$\frac{\partial C}{\partial t} + u \frac{\partial C}{\partial x} + v \frac{\partial C}{\partial y} = D_B \left(\frac{\partial^2 C}{\partial x^2} + \frac{\partial^2 C}{\partial y^2} \right) + \left(\frac{D_T}{T_0} \right) \left(\frac{\partial^2 T}{\partial x^2} + \frac{\partial^2 T}{\partial y^2} \right), \quad (3.14)$$

here u , v denote the velocities along the x - and y - directions respectively, α_1 is the second grade fluid parameter, σ_m is the electrical conductance, p is the pressure, ρ_f is the base fluid density, ρ_p is the density of the nano material particles, $(c_p)_f$ is the specific heat of the base fluid, α_f is the thermal diffusivity of base fluid, ν is kinematic viscosity, T is the temperature, C the concentration field, T_w, C_w are the temperature and concentration respectively at wall, T_0, C_0 the ambient fluid temperature and concentration respectively, D_B the Brownian diffusion coefficient, D_T is the thermophoretic diffusion coefficient, $\tau = \frac{(\rho c_p)_p}{(\rho c_p)_f}$ is the quotient between the effective heat capacity of the nanoparticle material and heat capacity of the fluid with ρ being the density, c_p is the volumetric volume expansion coefficient and q_r is the radiation heat flux.

The assumed boundary conditions for unsteady squeezed flow are

$$\begin{aligned} u &= U_0 = \frac{ax}{(1-\gamma t)}, \quad v = 0, \quad T = T_0, \quad C = C_0 \quad \text{at} \quad y = 0, \\ u &\rightarrow 0, \quad v = v_h = -\frac{\gamma}{2} \sqrt{\frac{v}{a(1-\gamma t)}}, \quad T \rightarrow T_0 + \frac{T_0}{(1-\gamma t)}, \quad C \rightarrow C_0 + \frac{C_0}{(1-\gamma t)} \quad \text{as} \quad y \rightarrow h(t), \end{aligned} \quad (3.15)$$

The Rosseland [26] approximation of radiation for an optically thick media and provides the net radiation heat flux

$$q_r = -\frac{4}{3\alpha_R} \text{grad}(e_b), \quad (3.16)$$

where $\alpha_R [m^{-1}]$ is the Rosseland mean absorption coefficient and $e_b [Wm^{-2}]$ is the black-

body emissive power which is given in terms of the absolute temperature T by the Stefan-Boltzmann radiation law, $e_b = \sigma_{SB}T^4$, with the Stefan-Boltzmann constant $\sigma_{SB} = 5.6697 \times 10^{-8}Wm^{-2}K^{-4}$.

For squeezing flow over a hot surface equation (3.16) of the net radiation heat flux absorbed in the fluid is reduces to

$$q_r = -\frac{16\sigma_{SB}}{3\alpha_R}T^3\frac{dT}{dy}, \quad (3.17)$$

T^4 is expressed as a linear function of temperature by using Taylor series expansion about T_0 is

$$T^4 = 4T_0^3T - 3T_0^4. \quad (3.18)$$

Introducing the following transformations [24],

$$\begin{aligned} \eta &= \sqrt{\frac{a}{v(1-\gamma t)}}y, \quad u = \frac{ax}{(1-\gamma t)}f'(\eta), \quad v = -\sqrt{\frac{av}{(1-\gamma t)}}f(\eta), \\ T &= T_0 + \frac{T_0}{(1-\gamma t)}\theta(\eta), \quad C = C_0 + \frac{C_0}{(1-\gamma t)}\phi(\eta). \end{aligned} \quad (3.19)$$

Making use of Eq. (3.19), Equation of continuity (3.1) is identically satisfied and Eqs. (3.11) to (3.15) along with (3.17) and (3.18) take the following form

$$f'''' - f'f'' + ff'' - \frac{Sq}{2}(\eta f'''' + 3f'') + \beta \left[f'f'''' - ff'''' + \frac{Sq}{2}(5f'''' + \eta f''''') \right] - M^2 f'' - \lambda(\theta' + N\phi') = 0, \quad (3.20)$$

$$(1 + Rd(\theta w)^3)\theta'' + Pr(f\theta' - \frac{Sq}{2}(2\theta + \eta\theta') + Nb\theta'\phi' + Nt(\phi')^2) = 0, \quad (3.21)$$

$$\phi'' + Pr Le(f\phi' - \frac{Sq}{2}(2\phi + \eta\phi')) + \frac{Nt}{Nb}\theta'' = 0, \quad (3.22)$$

$$f(0) = 0, \quad f(1) = \frac{Sq}{2}, \quad f'(0) = 1, \quad f'(1) = 0, \quad (3.23)$$

$$\theta(0) = 0, \quad \theta(1) = 1,$$

$$\phi(0) = 0, \quad \phi(1) = 1. \quad (3.24)$$

In these expressions M is the magnetic parameter, β is the second grade parameter, Sq is squeezing parameter, λ is the mixed convection parameter, N_p is the Buoyancy ratio parameter, Gr is the Grashof number, Re is the Reynolds number, θw is the temperature parameter, Pr is the Prandtl number, Rd the thermal radiation effect, N_b is the Brownian motion parameter, N_t is the thermophoresis parameter, Le is the Lewis number. These parameters are defined in the following manner.

$$\left\{ \begin{array}{l} M^2 = \frac{\sigma_m H^2(t)}{\rho a}, \quad Sq = \frac{\gamma}{a}, \quad \beta = \frac{a\alpha_1}{\rho(1-\gamma t)}, \quad \lambda = \frac{Gr}{Re^2}, \\ Gr = \frac{g\beta_T(T_w - T_0)x^3}{\nu_f^2}, \quad Re = \frac{ax^2}{\nu_f(1-\gamma t)}, \quad N_p = \frac{\beta_T(T_w - T_0)}{\beta_C(C_w - C_0)}, \quad \theta w = \frac{T_w + T_0}{2T_0}, \\ Rd = \frac{16\sigma T_0^3}{3ka}, \quad Pr = \frac{\nu_f}{a}, \quad N_b = \frac{\tau D_B(C_w - C_0)}{\nu_f}, \quad N_t = \frac{\tau D_T(T_w - T_0)}{T_0 \nu_f}, \\ Le = \frac{a}{D_B}, \quad \tau = \frac{(\rho c_p)_f}{(\rho c_p)_s}. \end{array} \right.$$

Expressions for the local Nusselt number Nu_x and the local Sherwood number Sh_x are

$$C_f = \frac{(\tau_{xy})_{y=h(t)}}{\rho \nu_h^2}, \quad Nu_x = \frac{xq_i}{k(T_w - T_0)}, \quad Sh_x = \frac{xj_m}{D_B(C_w - C_0)}. \quad (3.25)$$

Here τ_{xy} is the wall shear stress, q_i and j_m are the heat flux and mass flux, respectively.

$$\left\{ \begin{array}{l} \tau_{xy} = \mu \left(\frac{\partial u}{\partial y} + \frac{\partial v}{\partial x} \right) + \alpha 1 \left[\begin{array}{l} \frac{\partial^2 u}{\partial t \partial y} + \frac{\partial^2 v}{\partial t \partial x} + u \left(\frac{\partial^2 u}{\partial x \partial y} + \frac{\partial^2 v}{\partial x^2} \right) \\ + v \left(\frac{\partial^2 u}{\partial y^2} + \frac{\partial^2 v}{\partial x \partial y} \right) + \frac{\partial u}{\partial x} \left(\frac{\partial u}{\partial y} - \frac{\partial v}{\partial x} \right) + \frac{\partial v}{\partial y} \left(\frac{\partial v}{\partial x} - \frac{\partial u}{\partial y} \right) \end{array} \right] \\ q_i = -K \frac{\partial T}{\partial y} \Big|_{y=h(t)} + q_r \Big|_{y=h(t)}, \quad j_m = -D_B \frac{\partial C}{\partial y} \Big|_{y=h(t)} \end{array} \right. \quad (3.26)$$

Following Kuznetsov and Nield [24] the equation (3.26) takes the following form,

$$\left\{ \begin{array}{l} Re^{-1/2} Nu_x = -(1 + (\theta w)^3 Rd) \theta'(1), \quad Re^{-1/2} Sh_x = -\phi'(1), \\ 2Re^{1/2} C_f = F''(1) + \beta [Sq \{3F''(1) + F'''(1)\} + 4F'(1)F''(1) - 2F(1)F'''(1)]. \end{array} \right. \quad (3.27)$$

where $Re = ax^2/\nu(1-\gamma t)$ is local Reynolds number based on the stretching velocity U_0 .

3.3 Homotopy analysis solutions

Rule of solution expression and subjected boundary conditions direct us to select the initial guesses and auxiliary linear operators as follows [1].

$$\begin{cases} f_0(\eta) = \eta - 2\eta^2 + \eta^3 + Sq(\frac{3}{2} - \eta), \theta_0(\eta) = \eta, \phi_0(\eta) = \eta, \\ \mathcal{L}_f = \frac{d^4 f}{d\eta^4}, \mathcal{L}_\theta = \frac{d^2 \theta}{d\eta^2}, \mathcal{L}_\phi = \frac{d^2 \phi}{d\eta^2}, \end{cases}$$

Here f_0, θ_0 and ϕ_0 stand for the initial guesses of f, θ and ϕ respectively, $\mathcal{L}_f, \mathcal{L}_\theta$ and \mathcal{L}_ϕ [1] the linear operators. The complete description is given in the book of Liao [17, 18].

If $p \in [0, 1]$ denoting the embedding parameter and \hbar_f, \hbar_θ and \hbar_ϕ denoting the non-zero auxiliary parameters then the generalized homotopic equations corresponding to equations (11–16) are

$$\begin{aligned} (1-p)\mathcal{L}_f[\hat{f}(\eta, p) - \hat{f}_0(\eta)] &= p\hbar_f \mathcal{N}_f[\hat{f}(\eta, p), \hat{\theta}(\eta, p), \hat{\phi}(\eta, p)], \\ (1-p)\mathcal{L}_\theta[\hat{\theta}(\eta, p) - \hat{\theta}_0(\eta)] &= p\hbar_\theta \mathcal{N}_\theta[\hat{f}(\eta, p), \hat{\theta}(\eta, p), \hat{\phi}(\eta, p)], \\ (1-p)\mathcal{L}_\phi[\hat{\phi}(\eta, p) - \hat{\phi}_0(\eta)] &= p\hbar_\phi \mathcal{N}_\phi[\hat{f}(\eta, p), \hat{\theta}(\eta, p), \hat{\phi}(\eta, p)], \end{aligned} \quad (3.28)$$

$$\begin{cases} \hat{f}(\eta; p)|_{\eta=0} = 0, \quad \frac{\partial \hat{f}(\eta; p)}{\partial \eta}|_{\eta=0} = 1, \quad \hat{f}(\eta; p)|_{\eta=1} = \frac{Sq}{2}, \quad \frac{\partial \hat{f}(\eta; p)}{\partial \eta}|_{\eta=1} = 0, \\ \hat{\theta}(\eta; p)|_{\eta=0} = 0, \quad \hat{\theta}(\eta; p)|_{\eta=1} = 1, \quad \hat{\phi}(\eta; p)|_{\eta=0} = 0, \quad \hat{\phi}(\eta; p)|_{\eta=1} = 1, \end{cases} \quad (3.29)$$

$$\begin{aligned} \mathcal{L}_f[f_m(\eta) - \chi_m f_{m-1}(\eta)] &= \hbar_f \mathcal{R}_m^f(\eta), \\ \mathcal{L}_\theta[\theta_m(\eta) - \chi_m \theta_{m-1}(\eta)] &= \hbar_\theta \mathcal{R}_m^\theta(\eta), \\ \mathcal{L}_\phi[\phi_m(\eta) - \chi_m \phi_{m-1}(\eta)] &= \hbar_\phi \mathcal{R}_m^\phi(\eta), \end{aligned} \quad (3.30)$$

$$\begin{aligned} f_m(0) &= f'_m(0) = f_m(1) = f'_m(1) = 0, \\ \theta_m(0) &= \theta_m(1) = 0, \phi_m(0) = 0 = \phi_m(1), \end{aligned} \quad (3.31)$$

$$\begin{aligned}
\mathcal{N}_f[\hat{f}(\eta, p), \hat{\theta}(\eta, p), \hat{\phi}(\eta, p)] &= \frac{\partial^4 \hat{f}(\eta; p)}{\partial \eta^4} - \frac{\partial \hat{f}(\eta; p)}{\partial \eta} \frac{\partial^2 \hat{f}(\eta; p)}{\partial \eta^2} + \hat{f}(\eta, p) \frac{\partial^3 \hat{f}(\eta; p)}{\partial \eta^3} \\
&- \frac{Sq}{2} \left(\eta \frac{\partial^3 \hat{f}(\eta; p)}{\partial \eta^3} + 3 \frac{\partial^2 \hat{f}(\eta; p)}{\partial \eta^2} \right) - M^2 \frac{\partial^2 \hat{f}(\eta; p)}{\partial \eta^2} \\
&- \lambda \left(\frac{\partial \hat{\theta}(\eta, p)}{\partial \eta} + N1 \frac{\partial \hat{\phi}(\eta, p)}{\partial \eta} \right) \\
&+ \beta \left[\begin{aligned} &\frac{\partial \hat{f}(\eta; p)}{\partial \eta} \frac{\partial^4 \hat{f}(\eta; p)}{\partial \eta^4} - \hat{f}(\eta, p) \frac{\partial^5 \hat{f}(\eta; p)}{\partial \eta^5} \\ &+ \frac{Sq}{2} \left(5 \frac{\partial^4 \hat{f}(\eta; p)}{\partial \eta^4} + \eta \frac{\partial^5 \hat{f}(\eta; p)}{\partial \eta^5} \right) \end{aligned} \right] \quad (3.32)
\end{aligned}$$

$$\begin{aligned}
\mathcal{N}_\theta[\hat{f}(\eta, p), \hat{g}(\eta, p), \hat{\theta}(\eta, p), \hat{\phi}(\eta, p)] &= (1 + Rd(\theta w)^3) \frac{\partial^2 \hat{\theta}(\eta, p)}{\partial \eta^2} + \Pr \left(\begin{aligned} &\hat{f}(\eta, p) \frac{\partial \hat{\theta}(\eta, p)}{\partial \eta} \\ &- \frac{Sq}{2} \left(2\hat{\theta}(\eta, p) + \eta \frac{\partial \hat{\theta}(\eta, p)}{\partial \eta} \right) \end{aligned} \right) \\
&+ \Pr \left(Nb \frac{\partial \hat{\theta}(\eta, p)}{\partial \eta} \frac{\partial \hat{\phi}(\eta, p)}{\partial \eta} + Nt \left(\frac{\partial \hat{\theta}(\eta, p)}{\partial \eta} \right)^2 \right), \quad (3.33)
\end{aligned}$$

$$\mathcal{N}_\phi[\hat{f}(\eta, p), \hat{\theta}(\eta, p), \hat{\phi}(\eta, p)] = \frac{\partial^2 \hat{\phi}(\eta, p)}{\partial \eta^2} + \Pr Le \left(\begin{aligned} &\hat{f}(\eta, p) \frac{\partial \hat{\phi}(\eta, p)}{\partial \eta} - \\ &\frac{Sq}{2} \left(2\hat{\phi}(\eta, p) + \eta \frac{\partial \hat{\phi}(\eta, p)}{\partial \eta} \right) \end{aligned} \right) + \frac{Nt}{Nb} \frac{\partial^2 \hat{\theta}(\eta, p)}{\partial \eta^2}, \quad (3.34)$$

$$\begin{aligned}
\mathcal{R}_m^f(\eta) &= f_{m-1}'''' - \frac{Sq}{2} (\eta f_{m-1}'''' + 3f_{m-1}'') + \beta \frac{Sq}{2} (5f_{m-1}'''' + \eta f_{m-1}''''') \\
&- M^2 f_{m-1}'' - \lambda(\theta'_{m-1} + N\phi'_{m-1}) \\
&+ \sum_{k=0}^{m-1} \left(\begin{aligned} &\beta (f'_{m-1-k} f_k'''' - f_{m-1-k} f_k''''') \\ &- f'_{m-1-k} f_k'' + f_{m-1-k} f_k''' \end{aligned} \right), \quad (3.35)
\end{aligned}$$

$$\mathcal{R}_m^\theta(\eta) = (1 + Rd(\theta w)^3) \theta_{m-1}'' - \Pr \frac{Sq}{2} (2\theta_{m-1} + \eta \theta'_{m-1}) + \Pr \sum_{k=0}^{m-1} \left(\begin{aligned} &f_{m-1-k} \theta'_k + Nb(\phi'_{m-1-k} \theta'_k) \\ &+ Nt(\theta'_{m-1-k} \theta'_k) \end{aligned} \right), \quad (3.36)$$

$$\mathcal{R}_m^\phi(\eta) = \phi_{m-1}'' - \Pr Le \frac{Sq}{2} (2\phi_{m-1} + \eta \phi'_{m-1}) + Le \sum_{k=0}^{m-1} f_{m-1-k} \phi'_k + \frac{Nt}{Nb} \theta_{m-1}'', \quad (3.37)$$

$$\chi_m = \begin{cases} 0, & m \leq 1 \\ 1, & m > 1. \end{cases} \quad (3.38)$$

Expanding \hat{f} , $\hat{\theta}$ and $\hat{\phi}$ using the Maclaurin's series about p we have

$$\begin{aligned} \hat{f}(\eta; p) &= f_0(\eta) + \sum_{m=1}^{\infty} f_m(\eta)p^m, \\ \hat{\theta}(\eta; p) &= \theta_0(\eta) + \sum_{m=1}^{\infty} \theta_m(\eta)p^m, \\ \hat{\phi}(\eta; p) &= \phi_0(\eta) + \sum_{m=1}^{\infty} \phi_m(\eta)p^m, \end{aligned} \quad (3.39)$$

$$\begin{aligned} f_m(\eta) &= \frac{1}{m!} \left. \frac{\partial^m \hat{f}(\eta; p)}{\partial p^m} \right|_{p=0}, \\ \theta_m(\eta) &= \frac{1}{m!} \left. \frac{\partial^m \hat{\theta}(\eta; p)}{\partial p^m} \right|_{p=0}, \\ \phi_m(\eta) &= \frac{1}{m!} \left. \frac{\partial^m \hat{\phi}(\eta; p)}{\partial p^m} \right|_{p=0}, \end{aligned} \quad (3.40)$$

When $p = 0$ and $p = 1$ then

$$\begin{aligned} \hat{f}(\eta; 0) &= f_0(\eta), \quad \hat{f}(\eta; 1) = f(\eta), \\ \hat{\theta}(\eta; 0) &= \theta_0(\eta), \quad \hat{\theta}(\eta; 1) = \theta(\eta), \\ \hat{\phi}(\eta; 0) &= \phi_0(\eta), \quad \hat{\phi}(\eta; 1) = \phi(\eta). \end{aligned} \quad (3.41)$$

and the auxiliary parameters have been selected in such a manner that

$$\begin{aligned} f(\eta) &= f_0(\eta) + \sum_{m=1}^{\infty} f_m(\eta), \\ \theta(\eta) &= \theta_0(\eta) + \sum_{m=1}^{\infty} \theta_m(\eta), \\ \phi(\eta) &= \phi_0(\eta) + \sum_{m=1}^{\infty} \phi_m(\eta). \end{aligned} \quad (3.42)$$

We express the general solutions [27] of Eqs. (22) and (23)

$$\begin{aligned}
f_m(\eta) &= f_m^*(\eta) + C_1 + C_2\eta + C_3\eta^2 + C_4\eta^3, \\
\theta_m(\eta) &= \theta_m^*(\eta) + C_5 + C_6\eta, \\
\phi_m(\eta) &= \phi_m^*(\eta) + C_7 + C_8\eta,
\end{aligned} \tag{3.43}$$

in which $f_m^*(\eta)$, $\theta_m^*(\eta)$ and $\phi_m^*(\eta)$ denote the special solutions. Which are obtained with the help of MATHEMATICA and are discussed in the next section.

3.4 Convergence of the homotopy solutions

The convergence of the parametric valves are shown by OHAM, listed in below table [28].

$\frac{values \rightarrow}{order \downarrow}$	h_f	h_θ	h_ϕ	ϵ_m^t
2	-0.6335	-0.676585	-0.485469	0.0769792
4	-0.811348	-0.838445	-1.00871	0.000410105
6	-0.815009	-0.795099	-1.02461	$4.31758 * 10^{-7}$
8	-0.887184	-0.745552	-1.09382	$3.09281 * 10^{-9}$
10	-0.737516	-0.84729	-1.01794	$2.0372 * 10^{-11}$

Table.1 for average residual square errors (ϵ_m^t).

$\frac{values \rightarrow}{order \downarrow}$	h_f	h_θ	h_ϕ	ϵ_m^f	ϵ_m^θ	ϵ_m^ϕ
2	-0.6335	-0.676585	-0.485469	$1.2325 * 10^{-23}$	$4.2165 * 10^{-23}$	$1.8664 * 10^{-21}$
4	-0.811348	-0.838445	-1.00871	$8.23472 * 10^{-25}$	$1.40631 * 10^{-23}$	$2.01912 * 10^{-22}$
6	-0.815009	-0.795099	-1.02461	$9.85324 * 10^{-25}$	$1.07534 * 10^{-22}$	$4.85743 * 10^{-24}$
8	-0.887184	-0.745552	-1.09382	$1.26359 * 10^{-25}$	$1.23022 * 10^{-23}$	$8.93886 * 10^{-23}$
10	-0.737516	-0.84729	-1.01794	$3.3253 * 10^{-25}$	$2.55126 * 10^{-24}$	$7.66172 * 10^{-23}$

Table.2 shows individual residual square errors for ϵ_m^f , ϵ_m^θ and ϵ_m^ϕ .

Graphical representation for the 10th order approximation us given in the following figure.

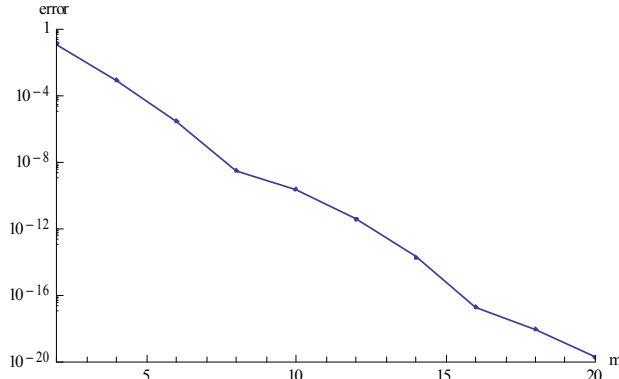


Fig. 3.1 Graph for 8th order approximations.

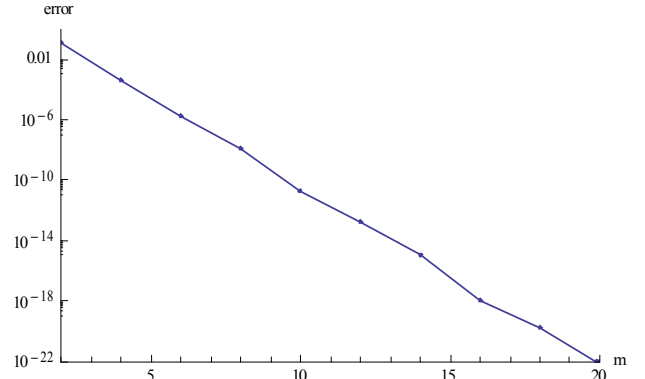


Fig. 3.2 Graph for 10th order approximations.

Here ϵ_m^ϕ is the total discrete squared residual error.

$$\epsilon_m^t = \epsilon_m^f + \epsilon_m^\theta + \epsilon_m^\phi.$$

Here the ϵ_m^ϕ is used to get the optimal convergence control parameters.

3.5 Results and discussions

This section concern with the effects of different parameters on the flow and heat transfer. For this purpose Fig.3.3 – 3.22 are plotted. The velocity, temperature and concentration profiles beside η are are designed for different values of all parameter used in the present model. Fig.3.3 – 3.5 shows the influence of second grade parameter β . It is shown that for $0 \leq \eta \leq 0.47$, the boundary layer thickness increases and for $0.47 \leq \eta \leq 1$, the boundary layer thickness reduces. However in Fig.3.4 – 3.5 the surface temperature and concentration reduces as β increases. These increase in velocity profile and decrease in temperature and concentration profiles are due to the viscoelastic effect and permeability of the wall. Fig.3.6 – 3.7 shows the effects of mixed convection parameter λ and the Buoyancy force parameter N_p on the velocity profile $f'(\eta)$. With the increase in mixed convection parameter λ and the Buoyancy force parameter N_p , the magnitude of velocity profile increases for $0 \leq \eta \leq 0.5$, and decreases for

$0.5 \leq \eta \leq 1.0$. A look up at over here λ and N_p are be contingent on buoyancy force. As a result, when we increase λ and N_p , ultimately the buoyancy force increasing, due to which the velocity and temperature profiles first increased and then decreased. Fig.3.8 the influence of magnetic parameter M . the plot show that for $0 \leq \eta \leq 0.45$, the boundary layer thickness reduces and for $0.45 \leq \eta \leq 1.0$, the boundary layer thickness increases. The physics of the magnetic parameter is that, an increase in M cause decrease in velocity. Subsequently the identical mass flow rate is compulsory because to the law of conservation of mass, hence by increasing M , we means, that decrease in the fluid velocity close to the wall will be recompensed by velocity of fluid close to the origin providing rise to a cross flow behavior. Fig.3.9 – 3.11 observe the behavior of squeezing parameter Sq on the velocity, temperature and concentration profiles. with the increase in squeezing parameter Sq we observe that the temperature profile decreases while the boundary layer thickness and concentration profile increases. The behavior of the Brownian motion parameter Nb is shown in Fig.3.12 – 3.13. It is shown that by increasing the parameter Nb the temperature and concentration profile increases. Fig.3.14 – 3.15 shows the effects of thermophoretic parameter Nt . Providing variation to Nt we see that the temperature profile increases while the concentration profile decreases. Fig.3.16 – 3.17 shows the influence of the Prandtl number on the temperature and concentration profiles. Due to large viscous dissipation effect, the Pr increases, where the temperature profile increases and the concentration profile decreases. Fig.3.18 – 3.19 shows the behavior of the radiation parameter Rd . The increase in radiation parameter Rd consequences the increases in temperature as will as in concentration profiles. With the increase in temperature parameter θw , the temperature as well as the concentration profiles increases, as shown in Fig.3.20 – 3.21. The influence of Lewis number Le is shown in Fig.3.22, it was observed that increasing the Lewis number Le the concentration

profile also decreases.

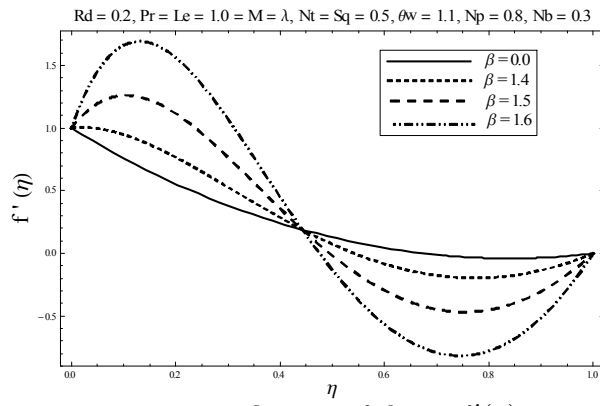


Fig. 3.3. Influence of β on $f'(\eta)$.

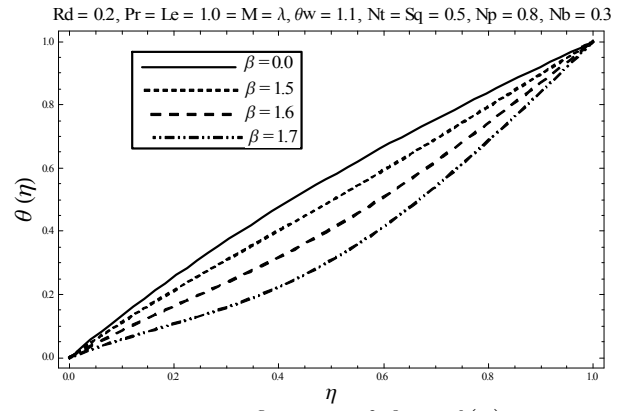


Fig.3.4. Influence of β on $\theta(\eta)$.

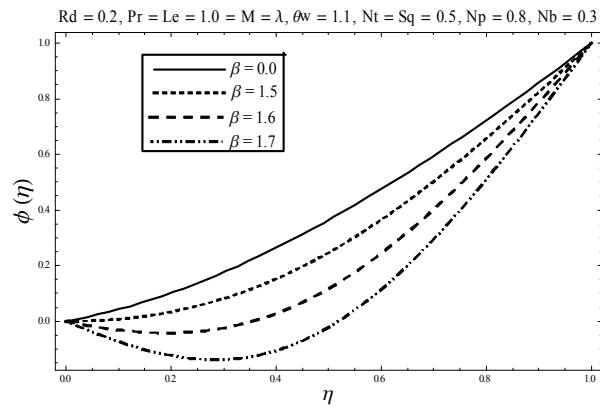


Fig. 3.5. Influence of β on $\phi(\eta)$.

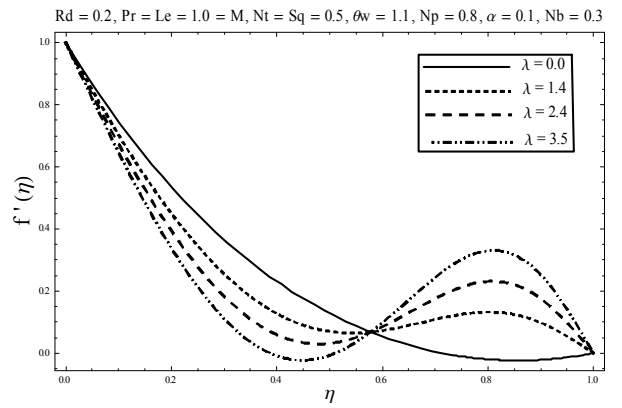


Fig. 3.6. Influence of λ on $f'(\eta)$.

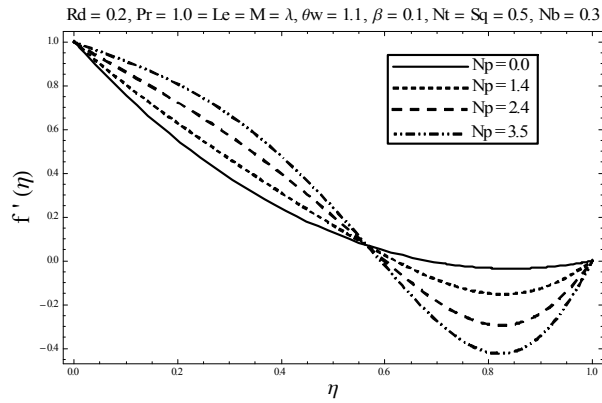


Fig. 3.7. Influence of N_p on $f'(\eta)$.

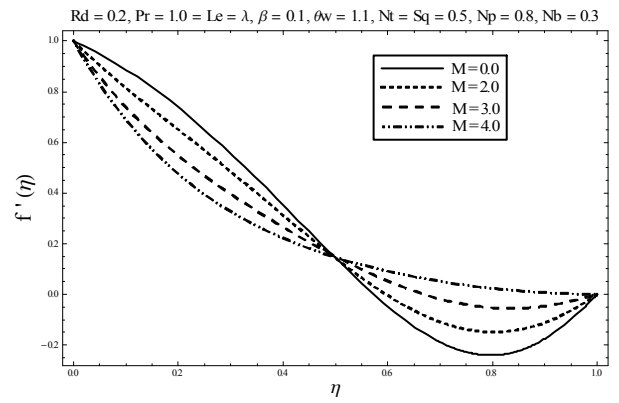


Fig. 3.8. Influence of M on $f'(\eta)$.

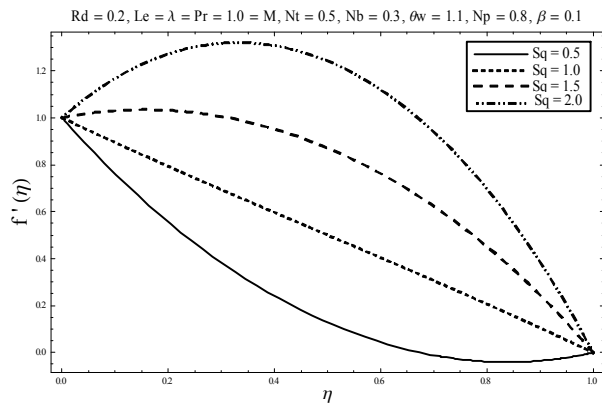


Fig. 3.9. Influence of Sq on $f'(\eta)$.

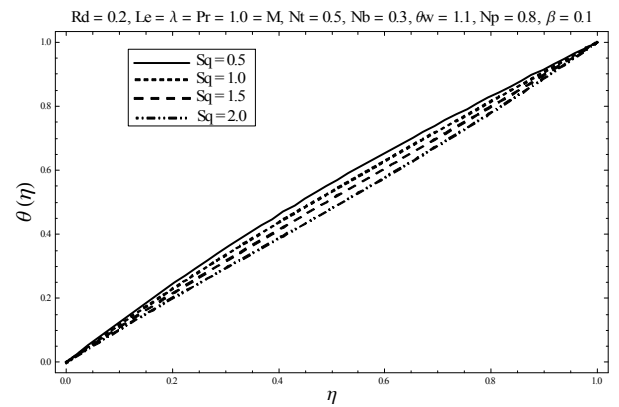


Fig. 3.10. Influence of Sq on $\theta(\eta)$.

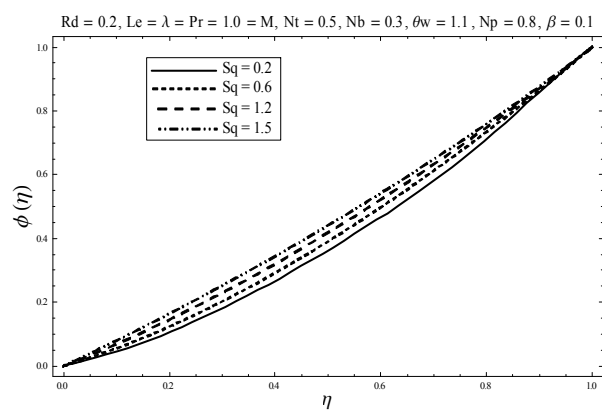


Fig. 3.11. Influence of Sq on $\phi(\eta)$.

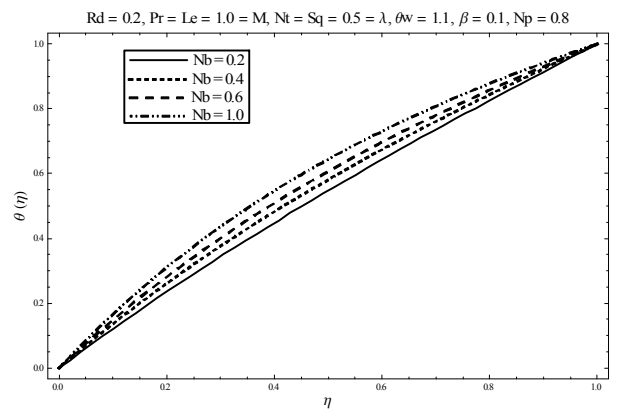


Fig. 3.12. Influence of Nb on $\theta(\eta)$.

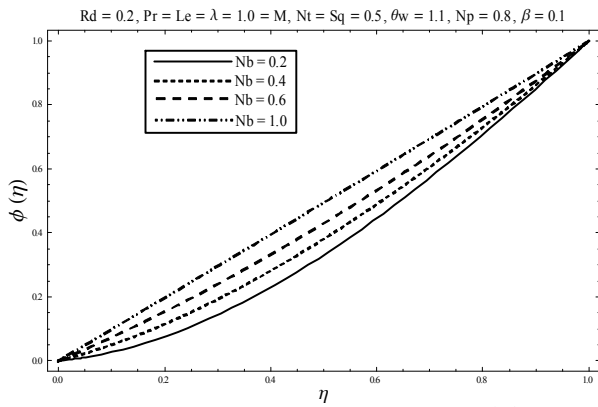


Fig. 3.13. Influence of Nb on $\phi(\eta)$.

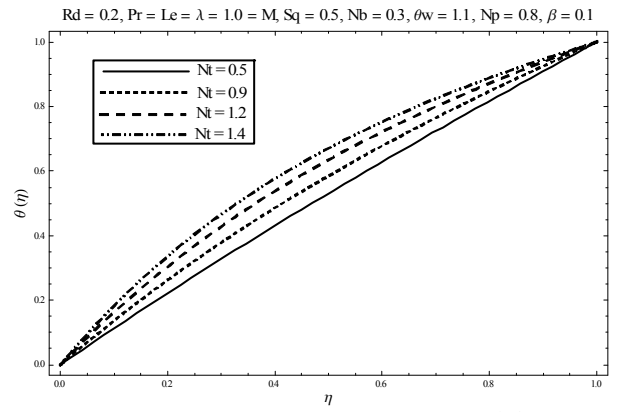


Fig. 3.14. Influence of Nt on $\theta(\eta)$.

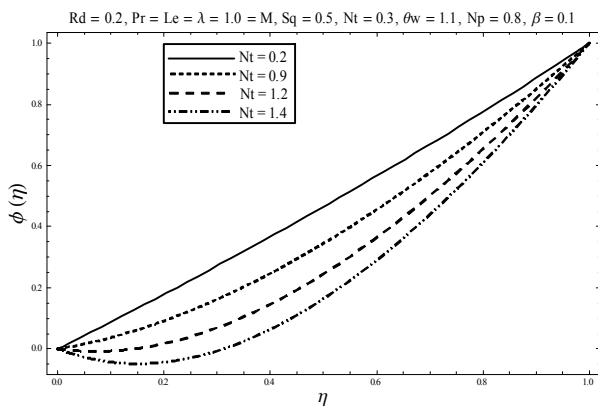


Fig. 3.15. Influence of Nt on $\phi(\eta)$.

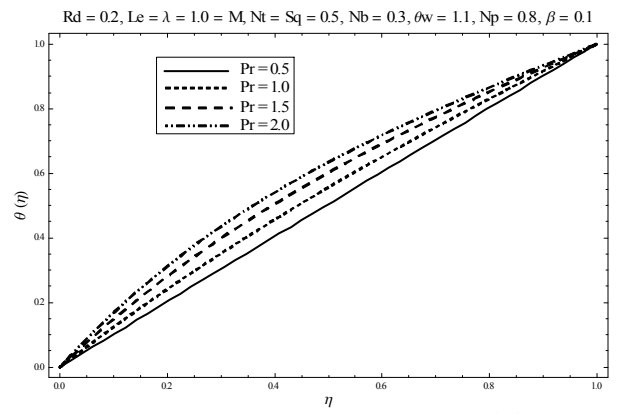


Fig. 3.16. Influence of Pr on $\theta(\eta)$.

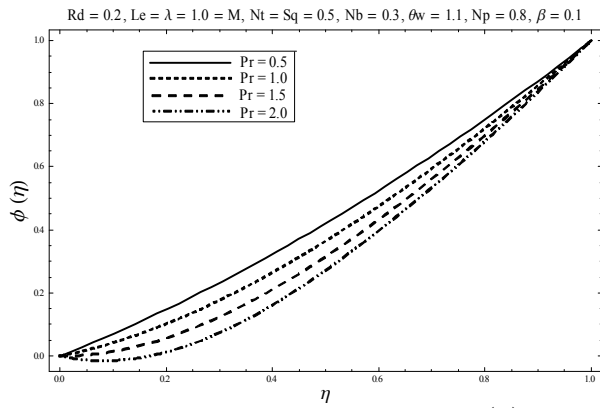


Fig. 3.17. Influence of Pr on $\phi(\eta)$.

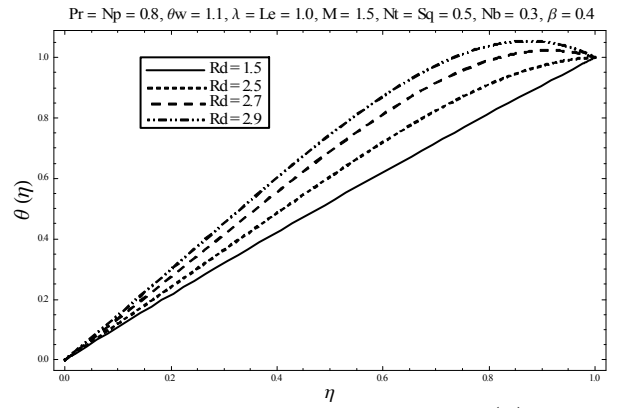


Fig. 3.18. Influence of Rd on $\theta(\eta)$.

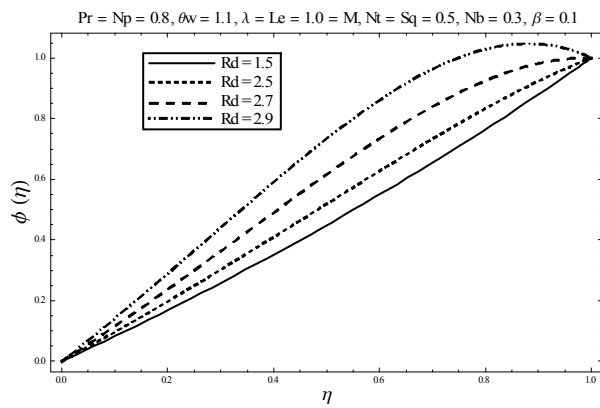


Fig. 3.19. Influence of Rd on $\phi(\eta)$.

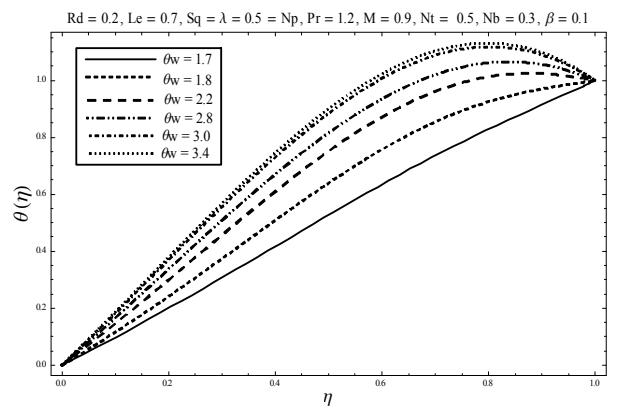


Fig. 3.20. Influence of θ_w on $\theta(\eta)$.

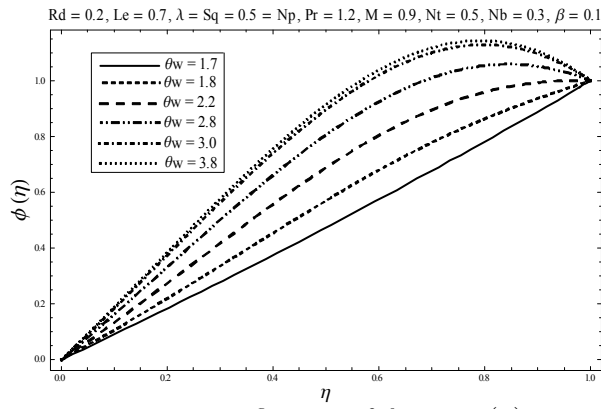


Fig. 3.21. Influence of θw on $\phi(\eta)$.

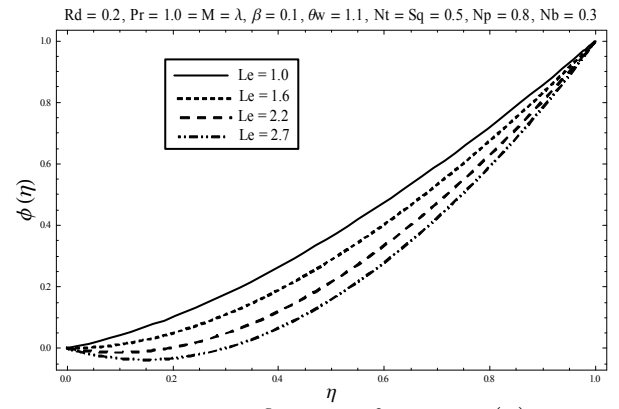


Fig. 3.22. Influence of Le on $\phi(\eta)$.

Table 2: Values for the skin friction coefficient, Nusselt number and Sherwood number for different values of $M, Sq, \beta, \lambda, N_p, \theta w, Rd, Nb, Nt, Le$ and Pr .

M	Sq	β	λ	N_p	θw	Rd	Nb	Nt	Le	Pr	$2Re^{\frac{1}{2}}C_f$	$-Re^{\frac{1}{2}}Nu_x$	$-Re^{\frac{1}{2}}Sh_x$
0.5	0.5	0.1	1.0	0.8	0.2	0.3	1.0	0.8	0.5	0.3	0.52381	0.93932	1.46665
1.0											0.59764	0.93873	1.46664
1.3											0.66543	0.93819	1.46663
1.0	0.0	0.1	1.0	0.8	0.2	0.3	1.0	0.8	0.5	0.3	1.46920	0.75550	1.58219
	0.4										0.91877	0.90332	1.48711
	0.6										0.25659	0.97356	1.44735
1.0	0.5	0.0	1.0	0.8	0.2	0.3	1.0	0.8	0.5	0.3	0.52342	1.11348	1.39642
		0.1									0.59766	1.11351	1.39643
		0.2									0.67206	1.11354	1.39643
1.0	0.5	0.1	0.5	0.8	0.2	0.3	1.0	0.8	0.5	0.3	0.54842	0.93912	1.46664
			0.9								0.58781	0.93881	1.46664
			1.3								0.62720	0.93850	1.46664
1.0	0.5	0.1	1.0	0.4	0.2	0.3	1.0	0.8	0.5	0.3	0.57578	1.11367	1.39647
				0.8							0.59766	1.11351	1.39643
				1.2							0.61952	1.11336	1.39639
1.0	0.5	0.1	1.0	0.8	0.0	0.3	1.0	0.8	0.5	0.3	0.59766	0.93765	1.46803
					0.5						0.59766	0.94259	1.46167
					0.8						0.59766	0.956081	1.44332
1.0	0.5	0.1	1.0	0.8	0.2	0.0	1.0	0.8	0.5	0.3	0.59766	0.78138	1.46803
						0.4					0.59766	1.09644	1.46526
						0.8					0.59766	1.41289	1.46252
1.0	0.5	0.1	1.0	0.8	0.2	0.3	0.2	0.8	0.5	0.3	0.59765	0.98439	1.54696

M	Sq	β	λ	N_p	θw	Rd	Nb	Nt	Le	Pr	$2Re^{\frac{1}{2}}C_f$	$-Re^{\frac{1}{2}}Nu_x$	$-Re^{\frac{1}{2}}Sh_x$
							0.5				0.59768	0.85289	1.39787
							1.0				0.59774	0.66839	1.33393
1.0	0.5	0.1	1.0	0.8	0.2	0.3	1.0	0.1	0.5	0.3	0.59761	1.12689	1.14429
								0.4			0.59765	0.98304	1.35189
								0.8			0.59772	0.81627	1.92756
1.0	0.5	0.1	1.0	0.8	0.2	0.3	1.0	0.8	0.9	0.3	0.59766	0.95804	1.09195
									1.2		0.59766	0.93415	1.56189
									1.4		0.59765	0.92966	1.65772
1.0	0.5	0.1	1.0	0.8	0.2	0.3	1.0	0.8	0.5	0.7	0.59764	1.00398	1.38221
										1.0	0.59766	0.93873	1.46664
										1.5	0.59770	0.85130	1.57853

Table 2 demonstrates the numerical values of the skin friction coefficient, Nusselt number and Sherwood number for certain parameter. With the increase in $M, \beta, \lambda, N_p, Nb, Nt,$ and Pr, the C_f increases, while C_f decreases with the increase in Sq and Le . Increase in $M, \lambda, N_p, Nb, Nt, Le$ and Pr, the Nu_x is decreased, on the other hand Nu_x increases, by increasing $Sq, \beta, \theta w$ and Rd . Lastly increasing M, Sq, N_p, Rd and Nb , the Sh_x decreases and by the way Sh_x increases for increasing $\beta, \theta w, Nt, Le$ and Pr.

3.6 Concluding Remarks

The squeezing flow, heat transfer and Rosseland thermal radiation are analyzed over here. The central theme of the above scene are listed below.

► β the second grade parameter when increased, the surface temperature and concentration reduces while the boundary layer thickness first increased for $0 \leq \eta \leq 0.47$, and for $0.47 \leq \eta \leq 1$, the boundary layer thickness reduces.

► The increase in mixed convection parameter and the Buoyancy force parameter, the magnitude of velocity profile increases for $0 \leq \eta \leq 0.5$, and decreases for $0.5 \leq \eta \leq 1.0$. where the surface temperature and concentration remains unchanged.

► An increase in squeezing parameter, the boundary layer thickness and concentration

profile increases while the temperature profile decreases.

- ▶ With increment in Brownian motion parameter, the temperature and concentration profile increases.

- ▶ With increment in thermophoretic parameter, we see that the temperature profile increases while the concentration profile decreases.

- ▶ An increase in Prandtl number, the temperature profile increases and the concentration profile decreases.

- ▶ An increase in radiation parameter results the increases in temperature as well as in concentration profiles.

- ▶ An increase in temperature parameter, the temperature as well as the concentration profiles increases and for higher values of temperature parameter, the temperature and the concentration profiles goes to an asymptotic state.

- ▶ The influence of Lewis number have been observed that increasing the Lewis number, the concentration profile decreases.

Bibliography

- [1] J.J. Buongiorno, Convective Transport in Nanofluids. ASME. *Journal of Heat Transfer*. vol. 128, pp. 240 – 250, (2005).
- [2] M.N. Ozisik, Interaction of Radiation with Convection in Handbook of Singlephase Convective Heat Transfer, John Wiley & Sons, New York, (1987).
- [3] W.J. Smith, Effect of gas radiation in the boundary layer on aerodynamic heat transfer, *Journal of the Aeronautical Sciences*. vol. 20, pp. 579 – 580, (1952).
- [4] R. Viskanta, R.J. Grosh, Boundary layer in thermal radiation absorbing and emitting media, *International Journal of Heat and Mass Transfer*, vol. 5, pp. 795 – 806, (1962).
- [5] M. Molla, C.S. Suvash, M.A. Hossain, Radiation effect on free convection laminar flow along a vertical flat plate with streamwise sinusoidal surface temperature, *Mathematical and Computer Modelling*, vol. 53, pp. 1310 – 1319, (2011a).
- [6] A. V. Kuznetsov, D. A. Nield, Natural convective boundary-layer flow of a nanofluid past a vertical plate. *International Journal of Thermal science*. vol. 49, pp. 243 – 247, (2010).
- [7] R. U. Haq, S. Nadeem, Z. H. Khan and N. S. Akbar, Thermal radiation and slip effects on MHD stagnation point flow of nanofluid over a stretching sheet. *Physica E: Low – dimensional Systems and Nanostructures*, vol. 65, pp. 17 – 23, (2015).
- [8] S. Nadeem, S. Zaheer, and T. Fang, Effects of thermal radiation on the boundary layer flow of a Jeffrey fluid over an exponentially stretching surface. *Numerical Algorithms*, vol. 57.2, pp. 187 – 205, (2011).

- [9] S. Nadeem and R. U. Haq, Effects of thermal radiation for magnetohydrodynamic boundary layer flow of a nanofluid past a stretching sheet with convective boundary conditions. *Journal of Computational and Theoretical Nanoscience*. vol. 11, pp. 1 – 9, (2014).
- [10] P. S. Gupta, and A. S. Gupta, Heat and mass transfer on a stretching sheet with suction or blowing, *The Canadian Journal of Chemical Engineering*, vol. 55, pp.744–746, (1977).
- [11] C. K. Chen, and M. I. Char, Heat transfer of a continuous stretching surface with suction or blowing. *Journal of Mathematical Analysis and Applications*, vol. 135, pp. 568–580, (1988).
- [12] A. Pantokratoras, Natural convection along a vertical isothermal plate with linear and non-linear Rosseland thermal radiation. *International Journal of Thermal Sciences*. vol. 84, pp. 151 – 157, (2014).
- [13] M.A. Hossain, M.A. Alim, D.A.S. Rees, The effect of radiation on free convection from a porous vertical plate, *International Journal of Heat and Mass Transfer*, vol. 42, pp. 181 – 191, (1999).
- [14] M. Mustafa, A. Mushtaq, T. Hayat, B. Ahmad, Nonlinear radiation heat transfer effects in the natural convective boundary layer flow of nanofluid past a vertical plate, A numerical study, vol. e103946, (2014).
- [15] R. Mehmood, S. Nadeem and N. Akbar, Oblique stagnation flow of Jeffrey fluid over a stretching convective surface: optimal solution. *International Journal of Numerical Methods for Heat & Fluid Flow*. vol.25, pp. 3, (2015).
- [16] M. M. Rashidi, S. C. Rajvanshi, N. Kavyani, M. Keimanesh, I. Pop, B. S. Saini, Investigation of heat transfer in a porous annulus with pulsating pressure gradient by homotopy analysis method. *Arab Journal of Science and Engineering*. vol. 39, pp. 5113 – 5128, (2014).
- [17] S. J. Liao, Beyond perturbation: Introduction to homotopy analysis method, *Chapman and Hall, CRC Press, Boca Raton* (2003).

- [18] S. J. Liao, Homotopy analysis method in non-linear differential equations. *Springer and Higher Education Press, Heidelberg* (2012).
- [19] T. Hayat, M. Hussain, S. Nadeem, A. Alsaedi and S. Ubaidat, Squeezed flow and heat transfer in a second grade fluid over a sensor surface. *Journal of Thermal Science*, vol. 18, pp. 357 – 364, (2014).
- [20] T. Hayat, A. Qayyum and A. Alsaedi, Three dimensional mixed convection squeezing flow. *Journal of Applied Mathematics and Mechanics*. vol. 36, pp. 47 – 60, (2015).
- [21] O. Pourmehran, M. Rahimi-Gorji, M. Gorji-Bandpy, D.D. Ganji, Analytical investigation of squeezing unsteady nanofluid flow between parallel plates by LSM and CM. *Journal of Alexandria Engineering*, vol. 54, pp. 17 – 26, (2015).
- [22] T. Hayat, A. Qayyum and A. Alsaedi, MHD unsteady squeezing flow over a porous stretching plate. *Journal of The European Physical Plus*. vol. 36, pp. 128 – 157, (2013).
- [23] R. Cortell, MHD flow and mass transfer of an electrically conducting fluid of second grade in a porous medium over a stretching sheet with chemically reactive species. *Chemical Engineering and Processing Process Intensification*, vol. 46.8, pp. 721 – 728, (2007).
- [24] T. Hayat, A. Qayyum and A. Alsaedi, MHD unsteady squeezing flow over a porous stretching plate. *Journal of The European Physical Plus*. vol. 36, pp. 128 – 157, (2013).
- [25] S. Nadeem ad R. U. Haq, Effects of thermal radiation for magnetohydrodynamic boundary layer flow of a nanofluid past a stretching sheet with convective boundary conditions. *Journal of Computational and Theoretical Nanoscience*. vol. 11, pp. 1 – 9, (2014).
- [26] T. Hayat, S. Asad, M. Mustafa and A. Alsaedi, MHD stagnation-point flow of Jeffrey fluid over a convectively heated stretching sheet. *Journal of the Computers & Fluids*. vol. 108, pp. 179 – 185, (2015).
- [27] R. Bandelli and K. R. Rajagopal, Start–up flows of second grade fluids in domains with one finite dimension. *International Journal of Non – Linear Mechanics*. vol. 30(6), pp. 817 – 839, (1995).

- [28] S. Nadeem, and S. T. Hussain, Heat transfer analysis of Williamson fluid over exponentially stretching surface. *Journal of Applied Mathematics and Mechanics*. vol. 35(4), pp. 489–502, (2014).